Shahrood University of Technology

Journal of Mining and Environment (JME)

Journal homepage: www.jme.shahroodut.ac.ir

Iranian Society of Mining Engineering (IRSME)

Investigating Effect of Liner Type and Lifter Count on Kinetic, Potential, and Total Energies of Grinding Media in Industrial Ball Mills–Part 2: Similar Connected Lifters with Different Volumes

Sajad Kolahi, Mohammad Jahani Chegeni*, and Asghar Azizi

Faculty of Mining, Petroleum & Geophysics Eng., Shahrood University of Technology, Shahrood, Iran

Article Info

Received 24 July 2024

Received in Revised form 27 November 2024

Accepted 10 January 2025

Published online 10 January 2025

DOI: 10.22044/jme.2025.14803.2809

Keywords

Discrete element method

Industrial ball mills

Liner type

Lifter count

Kinetic and potential energies

Abstract

In Part 2 of this research work, five types of liners, i.e. wave, step, step@, ship-lap, and ship-lap@, are examined. These liners all have similar connected lifters with different volumes. Their difference is in the width, height, and type of the lifter profile. All the five liner types, from 8 to 64 lifters, are simulated using the Discrete Element Method (DEM). In this research work, for the first time, data from the sum of the kinetic and potential energies of individual balls (79,553 particles) are used to find the appropriate range for the number of lifters. In other words, the kinetic and potential energies of all particles within the system (inside the ball mill) are the basis for determining the appropriate number of lifters. The results suggest that for the wave liner, the appropriate range of the number of lifters is between 8 and 16, for the step, step@, and ship-lap liners; it is between 12 and 20, and for the ship-lap@ liner, it is between 8 and 20. In fact, using the data on the kinetic and potential energies of the balls inside the mill, it is possible to determine the appropriate range of the number of lifters, which is done for the first time in this study. In general, it is suggested that the data on the kinetic and potential energies of the balls can be used to determine the number of mill lifters, and unlike what has been done. So far, by other researchers, the number of mill lifters should not be determined solely by using its diameter or the dimensions of the lifters. Also, the effect of mill-rotation direction on the values of kinetic and potential energies in step and ship-lap liners is investigated. It is shown that the step@ and ship-lap@ liners transfer more energy to the balls than the step and ship-lap liners, and have a suitable direction of rotation.

1. Introduction

Grinding is the most prevalent process utilized to liberate the concentrate from the tailings [1]. This process consumes a good deal of energy in concentration plants. However, it is a low-efficiency process, where merely approximately 1% of the total energy is utilized to comminution. The concentration plants could save about 70% of the power involved in grinding processes if this power was reduced to its practical minimum power draw [2].

Ball mills are utilized in concentrate plants for size reduction. The comminution process in ball mills by its very nature is highly power intensive. For instance, a convenential 5-m diameter ball mill consumes about 3–4 MW power [3]. Ball milling is an indispensable constituent of concentrate plants, and is substantial in other industry domains. This requires to be accomplished as efficiently as achievable, maximizing the ball mill capacity, while minimizing the operating costs. These grinding processes routinely utilize only 1-5% of the applied power for particle breakage. Therefore, it is possible to improve them [4].

Ball mills have been broadly utilized in a large sum of industrial sectors for grinding of coarse particles. They have been employed for many years in the production of fines and in the latest steps of the comminution process, in which optimal levels

Corresponding author: M.Jahani@shahroodut.ac.ir *(M. Jahani Chegeni)*

for the particle sizes for the flotation process are obtained. Albeit this everywhere apparatus of relatively incomplex construction has been subjected to extensive investigations; this industry as yet encounters with a quite low power efficiency of the comminution process [5]. Of all comminution machines, ball mills consume the most energy in the mineral processing industries. The power draw usually depends on the charge fill level, the lifter geometry, and the mill speed. Various researches have addressed this problem considering different variables that may be thought to have a great impact on energy consumption of ball mills, through empirical formulas. However, the empirical formulas developed were not able to accommodate each parameter for calculating the power draw [6]. The mill rotation speed is one of the important parameters in ball mills, because it affects the dynamic motion of the balls within the mill. In turn, the motion of the balls affects the distribution of the forces, and thus the power draw of the mill [6].

The usual procedure in the industry has so far been to confide in experience for lifter selection, which confines the feasibility of implementation of innovative techniques, which can improve mill performance [7]. Lifters in ball mills not only guard the mill shell from the tough ambiance inside the mill, but also play a vital role in the grinding efficiency. Lifter design of ball mills determines the ball trajectory, and consequently, the milling efficiency [8].

The potential of *DEM* for the design and optimization of ball mills is unequivocally accepted by the mineral engineering community. The challenge is to effectively use the simulation tool to improve industrial practice [9]. *DEM* has made consequential influence on the operation and design of industrial-scale ball mills. The inner ball and particle motions can be facilely inspected. Subsequently, *DEM* empowers us to design and inspect mill inner parts through simulation [10]. There are several areas of application in the analysis of ball mills, where *DEM* is most effective. These include analysis of charge motion for improved plant operation, power draw prediction, liner, and lifter design and micro-scale modeling for calculation of size distribution [9]. There is no established technique to decide the shape and configuration of lifter bars of ball mills [9].

A good many of researchers have been working on simulating the tumbling ball mills using the *DEM* method, which were fully addressed in Part 1. In Part 2, only their titles are mentioned to avoid repetition, and the research results are not stated. Mishra and Rajamani were the first ones who studied the trajectory of the balls in industrial ball mills using *DEM*. They established a computer code consisting of *DEM* to model the ball motion inside a 55 cm ball mill [11]. In three collaborative research works, Mishra and Rajamani conducted numeric *DEM* simulation of ball motions inside a 4.75 m diameter ball mill with thirty lifters utilizing *DEM* [12–14]. Agrawala et al. investigated the mechanics of media motion in a 90-cm diameter ball mill using *DEM* [15]. Radziszewski compared three modelling approaches to *DEM* implementation to charge motion modelling inside a 12 m length ball mill with thirty-six lifters of two types of lifter profiles, i.e. rectangular Hi-lo lifters and 60° Hi-lo lifters [16]. Cleary took advantage of *DEM* to anticipate consumed energy of industrial-scale ball mills, and to investigate their affectability to operating conditions such as charge composition, motion, and behavior, as well as the lifter geometry [17, 18]. Also cleary simulated a 5 m diameter ball mill using *DEM,* and predicted particle flows inside the mill [4]. Monama and Moys utilized *DEM* to model the dynamics of ball mill startup. A 0.55 m diameter ball mill was investigated to carry out the experimental analyses [6]. Hlungwani et al. validated the results of *DEM* simulations by comparing them with charge motion in a transparent laboratory-scale ball mill [19]. Djordjevic scrutinized the influence of lifters on power draw of ball mills using *DEM* [20]. In another research work, Djordjevic compared the power draw modelling results using the *DEM* with the results derived from the widely used empirical model of Morrell [21]. One more time, Djordjevic calculated shear and normal stresses of lifters in ball mills using *DEM* [22]. Mishra reviewed computer simulation of industrial-scale tumbling mills by *DEM* in two parts [3, 9]. Powell and McBride illustrated the grinding regions (head, departure shoulder, center of circulation, equilibrium surface, bulk toe, and impact toe), and media motion inside ball mills [23]. Makokha and Moys evaluated the effect of lifter geometry and their profile design on kinetics of batch-scale ball-milling, and the milling throughput for optimization of the grinding performance using the mono-size quartz material as feed [24]. A novel procedure for optimization of the functioning and life of worn lifters in ball mills was presented by Makokha et al. [7]. Rezaeizadeh et al. showed that in order to achieve a higher impact frequency and amount of impact, which can lead to a higher overall efficiency, the mineral processing plant

engineer must increase the lifter count, lifter height, and mill speed, but must decrease the mill filling [25]. Pérez-Alonso and Delgadillo experimentally validated a 2D *DEM* code by analyzing digital snapshots of the ball velocity profiles. Also they measured the toe and shoulder angles and predicted power draw in ball mills [26]. In the early 1960s, Art MacPherson scrutinized the effect of lifter spacing to height ratios, and concluded that a ratio of 4:1 maximized grinding [10]. Yahyaei et al. extended an approach for designing lifters and functioning through scrutinizing the influence of relining effectiveness in an industrial case [8]. Bbosa et al. developed a novel methodology to determine and calculate power consumption of every individual size fraction of charge in ball mills [27]. Boemer and Ponthot experimental validated the *DEM* simulations of a 1:5-scale laboratory ball mill [28]. Peng et al. investigated the behavior of mono-sized iron ore particles as a charge inside a 0.52 m ball mill with single wave liner profile and twelve lifters using *DEM* [29]. Bian et al., utilizing *DEM* simulation, scrutinized the effect of lifter geometries and mill rotation speed on power consumption and particle trajectory as well as torque of a laboratory-scale ball mill [30]. Sun et al. studied the RPAS liners in ball mills [31]. Yin et al. investigated the impact behavior between different charges and lifters in a laboratory-scale ball mill [32]. Pedrayes et al., utilizing *DEM,* investigated frequency amplitude description of torque in a pilot-scale ball mill [2]. Li et al. studied the functioning of a particular 900 mm × 1800 mm ball mill with lifter structure based on *DEM* [33]. Panjipour and Barani, utilizing *DEM,* scrutinized the effect of ball size distribution on breakage mechanism, power consumption, and ball trajectory of a 25 cm ball mill [34]. Rosales-Marín et al. assessed the effect of lifter profile and their face angle and wear on power draw of a laboratory-scale ball mill as well as they measeard mill speed and breakage rate [1]. Lee et al. analyzed the grinding kinetics in a laboratory-scale 20 cm ball mill with six designed lifters (1cm-4lifters, 1cm-8lifters, 1cm-12 lifters, 2 cm-4lifters, 2cm-8 lifters, 2cm-12lifters) [35]. Li et al., utilizing *DEM,* investigated a ball mill with magnetic liners, and evaluated the charge trajectory and breakage effect [36]. Chimwani, and Bwalya utilized *DEM* to explore how shell liners of a ball mill may induce ball segregation [37]. Góralczyk et al. studied increasing energy efficiency and productivity of the comminution process in tumbling mills by indirect measurements of internal dynamics [5]. Shahbazi et al. presented a comprehensive review of the impact of various media shapes (spherical, cylpebs, eclipsoids, cube, worn ball, boulpebs, conipebs), and geometries on the functioning of ball mills [38]. AmanNejad and Barani carried out a broad survey to describe the role of mill rotation speed and ball size fractions, as well as the interactions of these two parameters on ball trajectory and power consumption in a laboratory-scale ball mill [39]. Kolahi et al. have investigated the effect of seven different types of liners on the performance of industrial scale ball mills [40]. Jahani Chegeni and Kolahi, by introducing a couple of new parameters, that is to say, *HH* (Head Height) and *IZL* (impact zone length), determined a proper range for the lifter number in pilot-scale ball mills using *DEM* [41]. Recently, Safa and Aissat proposed helical lifters to advance the ball mill performance [42].

In Part 2 of this research work, five other types of liners, i.e. wave, step, step@, ship-lap, and ship-lap@, are investigated. These liners all have similar connected lifters with different volumes. Their difference is in the width, height, and type of lifter profile. As the lifter count increases, their profile volume decreases. Step and step@ liners are geometrically similar, and their difference is in the mill rotation direction. This matter is also true for the ship-lap and ship-lap@ liners. First, all types of liners are simulated with eight lifters, using the Discrete Element Method (*DEM*). Then the lifter count is increased four by four to fill the entire wall of the mill with sixty-four lifters. Based on this, all liner types from 8 to 64 lifters are simulated. Similar to Part 1, the kinetic (*KE*) and potential (*PE*) energies as well as the sum of these two energies Total Energy (*TE*) of all the balls have been obtained throughout the simulation time from zero to thirteen seconds and in each time step. Also their corresponding graphs for all five types of liners and all lifter numbers from four upwards are drawn, and compared in detail. As previously mentioned, a good many of methods have been introduced by various researchers to calculate the energy consumption and power draw of ball mills such as the use of torque sensors, etc. However, the issue is that in none of the previous researches, the method and procedure of calculating the energy/power of the mills, whether by using *DEM* or by using other methods, has not been clearly and explicitly stated. In other words, researchers have only stated that the energy/power of a certain mill was calculated. But they have not mentioned anything about how to calculate it. Nonetheless, in the current research work, the *KE* and *PE* have

been accurately calculated according to the mass, coordinates, height, and speed of all the balls at any time step according to $KE = 1/2mV^2$ and $PE = mgh$ formulas, where, m is the mass of the ball (kg), V is the speed of the ball (m/s), g is the acceleration of gravity (m/s^2), and h is the height of the ball from the bottom of the mill (m). First, the *KE* and *PE* for a single ball are calculated. Then to calculate the *KE* and *PE* of all the balls, these values are added together to obtain the total *KE* and *PE*. Calculating the coordinates, height, and speed of all balls in all time steps and during the simulation time from zero to thirteen seconds for all types of liners and with the lifter count mentioned above, is a very time-consuming process, and took about two years, which has been done for the first time by the authors of this article. Also the effect of mill rotation direction on the values of *KE* and *PE* of balls in step and ship-lap liners are investigated. It is worth mentioning that, given the *KE* and *PE* of all balls, the optimal lifter count can be obtained for each type of liner. Also in order to investigate the effect of the direction of mill rotation on the Meskavan Company ball mill, which was validated in Part 1 of this research work, the values of *KE*, *PE*, and *TE* of the balls in Meskavan and Meskavan@ mills are compared. In the Meskavan mill, the mill rotates clockwise according to the design of the lifters. But in the Meskavan@, the mill rotates in a trigonometric direction contrary to the design of the lifters.

2. Ball Mill Configuration

In this research work, an industrial-scale ball mill with dimensions of 3.17 m × 5.70 m is investigated. Five types of liners, i.e. wave, step, step@, ship-lap, and Ship-lap@ were installed inside the mill. These liners all have similar connected lifters with different volumes. Their difference is in the width, height, and type of lifter profile. As the lifter count increases, their profile volume decreases. Step and step@ liners are geometrically similar, and their difference is in the mill rotation direction. This issue is also true for the ship-lap and ship-lap@ liners (Figures 1–3). First, all types of liners were simulated with eight lifters, utilizing the *DEM*. Then the lifter count was increased four by four to fill the entire wall of the mill with sixty-four lifters. Based on this, all liner types from 8 to 64 lifters were simulated (Figures 4–6). In total, 75 simulation runs were performed in Part 2 of this research work.

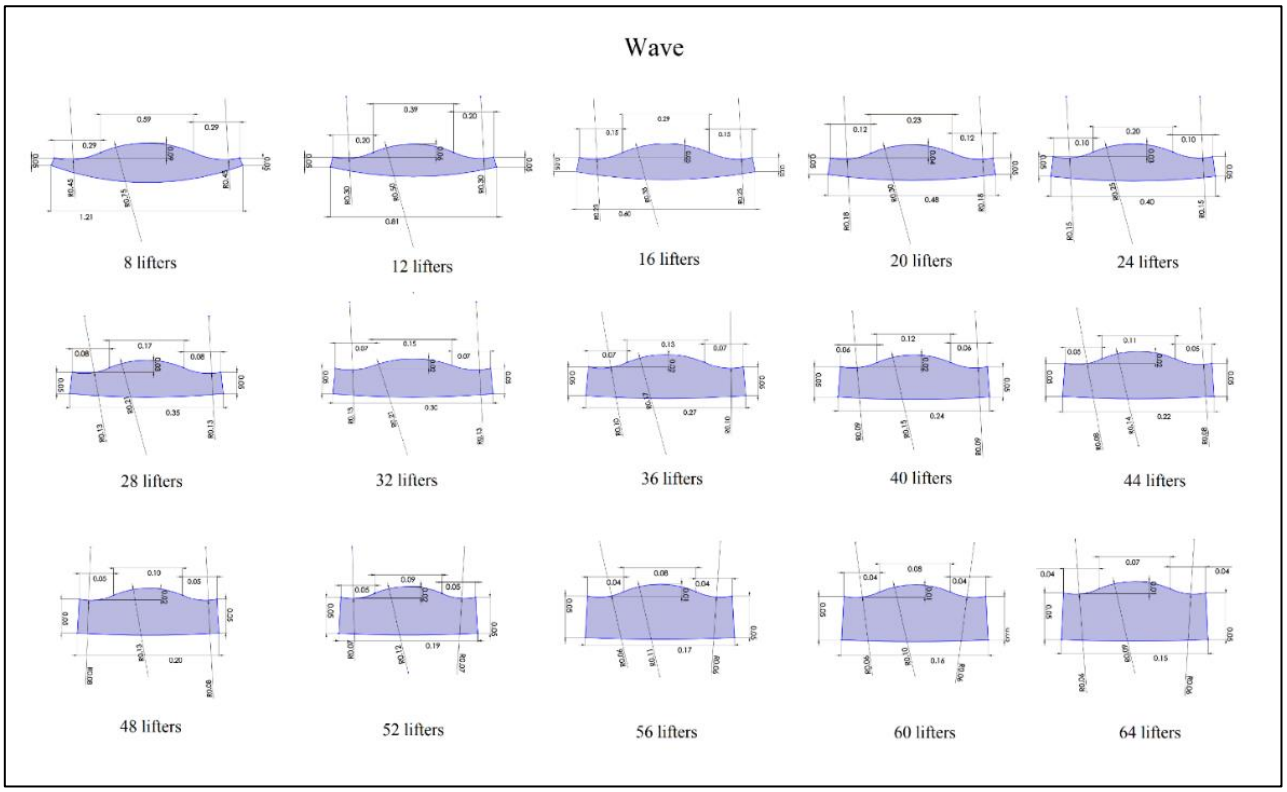

Figure 1. Detailed geometric specifications of 2D profiles of wave liner from 8 to 64 lifters.

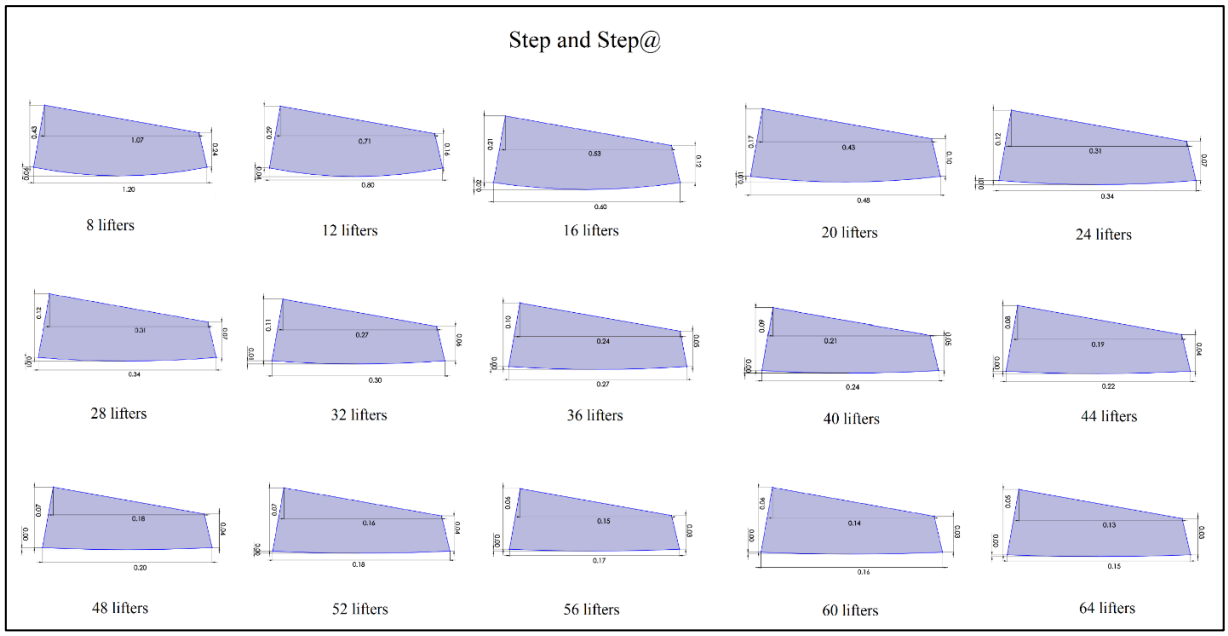

Figure 2. Detailed geometric specifications of 2D profiles of step and step@ liners from 8 to 64 lifters.

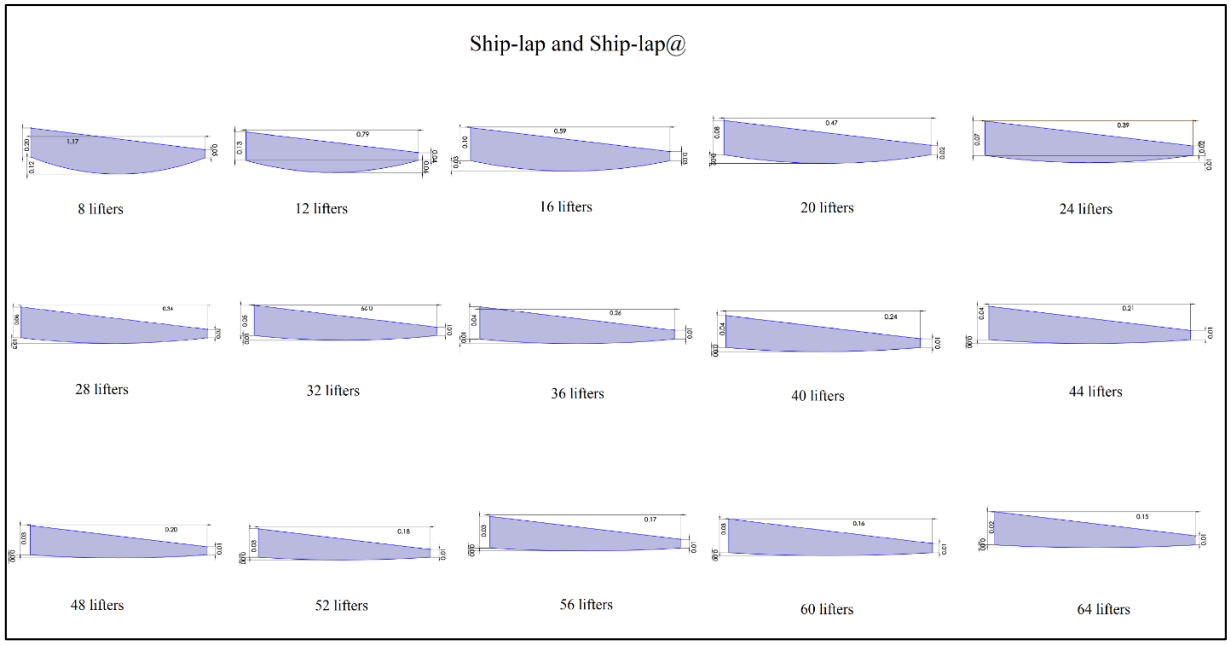

Figure 3. Detailed geometric specifications of 2D profiles of ship-lap and ship-lap@ liners from 8 to 64 lifters.

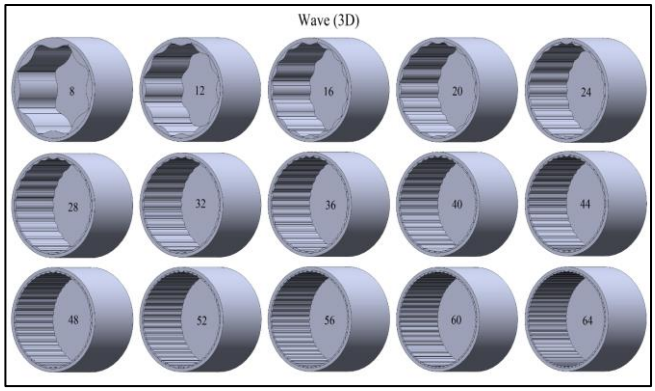

Figure 4. 3D geometries of industrial ball mills with wave liner from 8 to 64 lifters.

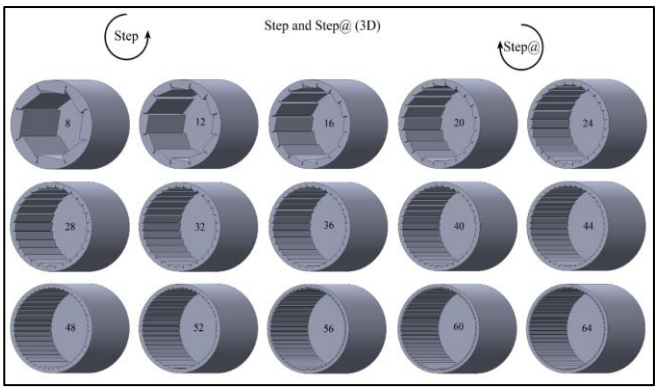

Figure 5. 3D geometries of industrial ball mills with step and step@ liners from 8 to 64 lifters.

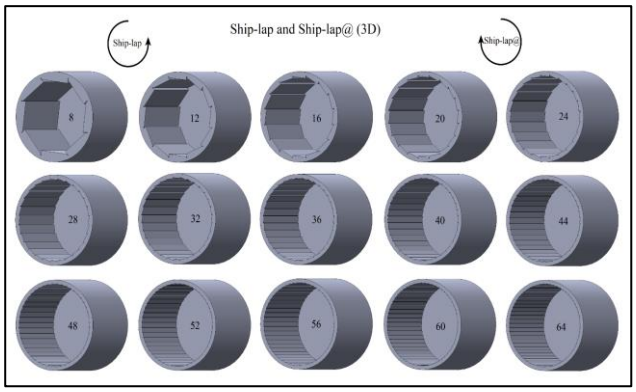

Figure 6. 3D geometries of industrial ball mills with the ship-lap and ship-lap@ liners from 8 to 64 lifters.

Detailed operating and geometric conditions, material properties, and calculations for these industrial scale ball mills are tabulated in Tables 1–3. It is worth noting that in this research work, all balls have the same diameter of 6 cm. The reason for keeping the ball diameter constant is to prevent the effect of changing their size on the *KE* and *PE* as well as the sum of these two energies of all the balls. Optimizing the ball size distribution for all liners studied in this research work is the subject of authors' future researches. In Table 3, the particle interaction distance (neighborhood), i.e. the distance that the particles exert a vertical and shear force on each other, is calculated as follows: One twentieth (5%) radius of the smallest particle (30 mm). It is noteworthy to mention that the material of the balls and walls of the mills used in these simulations is stainless steel. The parameters used in Tables 2 and 3, such as ball density, ball sliding friction coefficient, ball rolling friction coefficient, Poisson ratio, Young's modulus, and ball restitution coefficient, belong to stainless steel, and obtained from reputable internet websites. Table 4 shows the volume of a single lifter for the five types of liners investigated in this research work. As can be seen, as the lifter count increases, their volume decreases. Table 5 demonstrates the useful internal volume of all mills after installation of different lifter count for the five types of liners studied here. As can be seen again, by increase of the lifter count and decrease of their volume, the useful volume inside the mill increases.

Table 1. Dimensions and velocities of the industrial-scale ball mill.

Industrial scale ball mill	Value
Mill inside length (m)	5.70
Mill inside diameter (m)	3.17
Inside volume of no lifter mill (m^3)	44.98661 = 44.99
Critical speed (CS) (rpm)	23.99
Mill rotation speed (80% of CS) (rpm)	19.19
Mill rotation direction at wave, step, and ship-lap liners	Clockwise
Mill rotation direction at Step@ and Ship-lap@ liners	Counter-clockwise

Table 2. Calculations and specifications of *DEM* balls.

Ball diameter (cm)	6
Volume of a single ball (m^3)	$1.13097 \times 10^{-4} = 1.13 \times 10^{-4}$
Filling of mill ball charge (%)	40%
Volume of all balls (m^3)	40% /2 × 44.98661 = 8.99732 = 9.00
Number of balls in simulation	$8.99732/1.13097 \times 10^{-4} = 79553$
Ball density (kg/m^3)	8050
Total mass of balls (kg)	8050 × 8.99732 = 72428.44104 = 72428.44

Table 3. Parameters of *DEM* simulations.

DEM model details	Value
DEM spring constant (kg/m)	10^6
Ball sliding friction coefficient	0.5
Ball rolling friction coefficient	0.0015
Poisons ratio	0.285
Young's modulus (N/m^2)	1×10^9
Ball restitution coefficient	0.817
Time step (s)	$0.0001 = 10^{-4}$
Period of 80% CS	60/19.19 = 3.12681
Particle interaction distance (m)	$5\% \times 30 \text{ mm} = 15 \times 10^{-4}$

Table 4. Volume of a single lifter for five liner types studied here.

Lifter count		Volume of a single lifter (m^3)														
		8	12	16	20	24	28	32	36	40	44	48	52	56	60	64
Liner type	Wave	1.0830	0.4560	0.2850	0.1710	0.0900	0.0474	0.0249	0.0131	0.0069	0.0036	0.0019	0.0010	0.0005	0.0003	0.0001
	Step	2.5650	1.0830	0.5700	0.3990	0.1710	0.1140	0.0912	0.0741	0.0570	0.0456	0.0371	0.0296	0.0239	0.0200	0.0154
	Step@	2.5650	1.0830	0.5700	0.3990	0.1710	0.1140	0.0912	0.0741	0.0570	0.0456	0.0371	0.0296	0.0239	0.0200	0.0154
	Ship-lap	1.3110	0.5130	0.2850	0.1710	0.0969	0.0513	0.0285	0.0171	0.0091	0.0051	0.0029	0.0015	0.0010	0.0005	0.0003
	Ship-lap@	1.3110	0.5130	0.2850	0.1710	0.0969	0.0513	0.0285	0.0171	0.0091	0.0051	0.0029	0.0015	0.0010	0.0005	0.0003

Table 5. Useful internal volume of all mills after installation of different lifter count.

Lifter count		Mill inside volume (m^3)														
		8	12	16	20	24	28	32	36	40	44	48	52	56	60	64
Liner type	Wave	36.32	39.51	40.43	41.57	42.83	43.66	44.19	44.51	44.71	44.83	44.89	44.93	44.96	44.97	44.98
	Step	24.47	31.99	35.87	37.01	40.88	41.79	42.07	42.32	42.71	42.98	43.21	43.45	43.65	43.79	44.00
	Step@	24.47	31.99	35.87	37.01	40.88	41.79	42.07	42.32	42.71	42.98	43.21	43.45	43.65	43.79	44.00
	Ship-lap	34.50	38.83	40.43	41.57	42.66	43.55	44.07	44.37	44.62	44.76	44.85	44.91	44.93	44.95	44.97
	Ship-lap@	34.50	38.83	40.43	41.57	42.66	43.55	44.07	44.37	44.62	44.76	44.85	44.91	44.93	44.95	44.97

3. Results and Discussion

3.1. *DEM* simulations of industrial ball mills

Figure 7 illustrates *DEM* simulation legend for all simulations, conducted throughout this research work. Blue balls have the lowest speed, while red balls have the highest speed with a speed of about 4 m/s. The reason for the separate display of the legend is to preserve the symmetry in the simulation images and to reduce the size of the figures. All the snapshots for all the liners studied in this research were taken within 5 seconds after the mill came to its steady state. In all the simulations, the duration of the simulation was 13 seconds, and for most of the liners, the mill reached a steady state after 3 to 5 seconds. Therefore, for comparison, all snapshots were taken at 5 seconds.

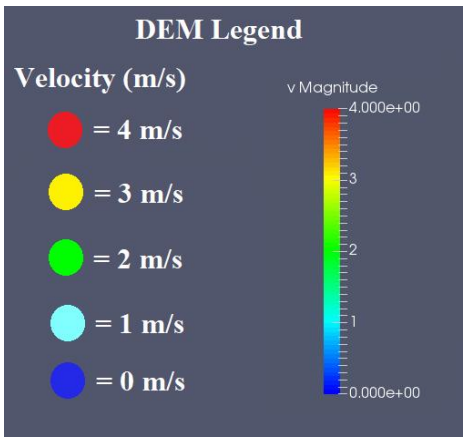

Figure 7. *DEM* simulation legend for all simulations.

Figure 8 demonstrates three-dimensional *DEM* simulation snapshots (front view) of industrial ball mills with wave liner from 8 to 64 lifters. As it can be seen, in all modes from 8 to 64 lifters, the wave liner does not have the ability to create cascading and cataracting motions for the balls. The reason is that this liner is smooth and without edges, which causes the balls to slide. In other words, the sliding friction between this liner and the balls is small. By increase of the lifter count from 8 to 64, the useful volume inside the mill has decreased. For example, in the 8-lifter mode, the useful volume inside the mill is about 36.32 m^3, which is about 20% less than the lifter-less mill with a volume of 44.99 m^3. In the 32-lifter mode, the useful volume inside the mill is about 44.19 m^3, which means about 2% reduction in volume compared to the lifter-less mill. From 36 to 64 lifters, practically increasing the lifter count does not affect the performance of the mill and it works, like a lifter-less mill. In general, it can be said that the wave liner is not suitable for installation in industrial ball mills, due to the inability to create an impact mechanism for the balls. However, in some industries such as the cement industry, where, an abrasion mechanism is required and the production of fines does not cause problems for the next stages of the process; this liner can be used.

Figure 9 demonstrates three-dimensional *DEM* simulation snapshots (front view) of industrial ball mills with step liner from 8 to 64 lifters. The rotation direction of the mill in this liner is of special importance due to its asymmetry. In step liner, the rotation direction of the mill is opposite to the design of its lifters, and is clockwise. In other words, the direction of rotation of the mill is deliberately chosen incorrectly. On the contrary, in step@ liner, the direction of rotation of the mill is in accordance with the design of its lifters and is counter-clockwise (Figure 10). The reason for this work is to compare and investigate the effect of the rotation direction of the mill on the motions of the balls in these asymmetric lifters. As can be seen from Figure 9, in the 8-lifter mode, due to the bulkiness of the lifters (the volume of a single lifter is about 2.565 m^3), the useful volume inside the mill has reached 24.47 m^3 from 44.99 m^3 in the lifter-less mode, that is it has decreased by about 46%. On the other hand, these bulky lifters bring the *KE* of the balls to about 241.79 kJ in this mode, which is about five times that of the

12-lifter mode (51.28 kJ). As a result, in this mode, the balls have caused the wall of the mill to tear and some of them (862 balls) have come out of the mill. Therefore, it is practically impossible to install step liner with 8 lifters in this mill. Despite the incorrect rotation direction of the mill, due to the edge of its lifters, cascading and cataracting motions have been created for the balls in the 12–44 lifter modes. However, in the 48 to 64 lifter modes, these motions have gradually disappeared, which indicates the insignificant influence of the lifters on the motions of the balls in these modes. In general, it can be said that step liner is an appropriate liner for installation in industrial scale ball mills, because both its height and width are suitable. Also, its edge (unlike the wave liner) creates the required sliding friction between the balls and the lifters.

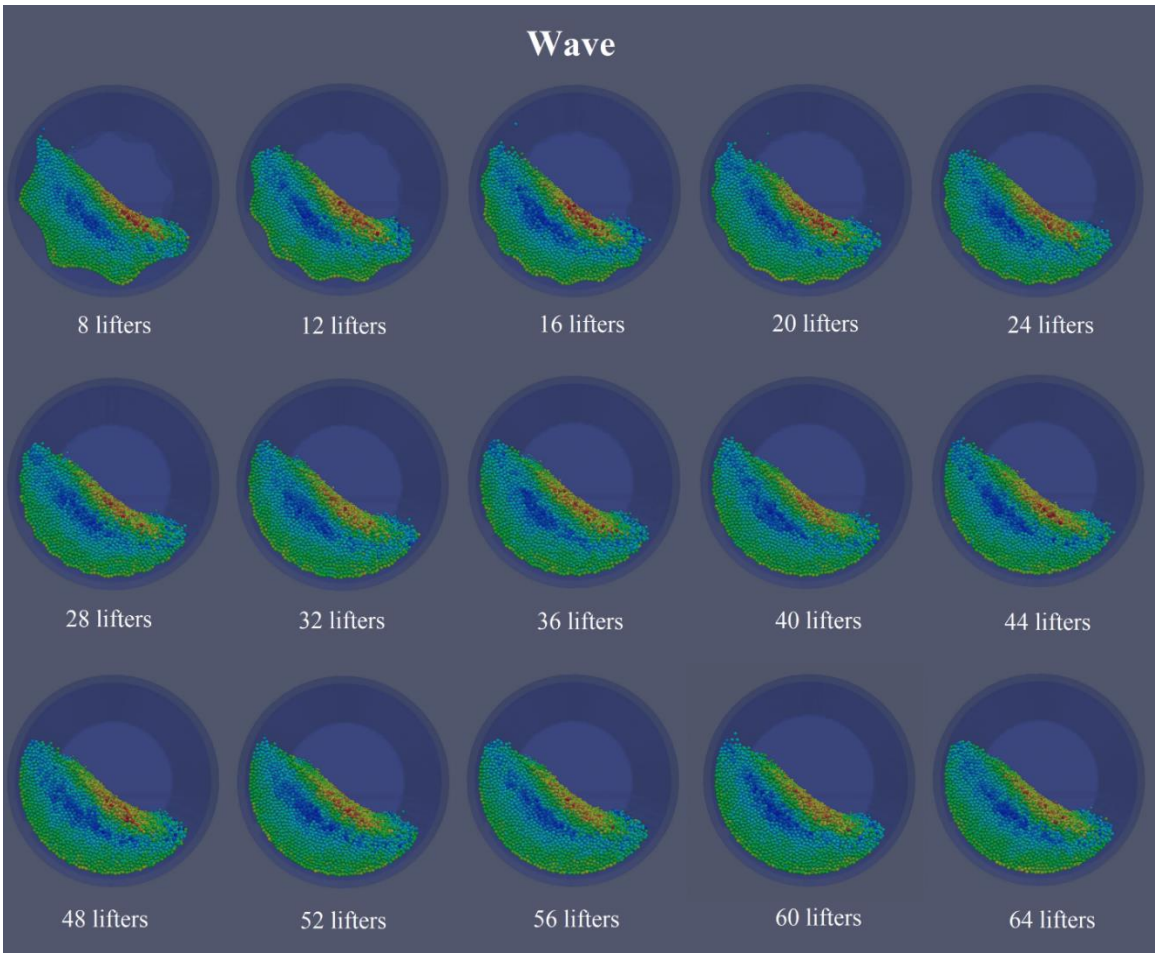

Figure 8. 3D *DEM* simulation snapshots (front view) of industrial ball mills with wave liner from 8 to 64 lifters.

Figure 10 demonstrates three-dimensional *DEM* simulation snapshots (front view) of industrial ball mills with step@ liner from 8 to 64 lifters. Step@ liner in all modes (from 8 to 64 lifters) has the same profile as step liner. Their difference is in the direction of rotation of the mill. In the step@ liner, the mill rotates in the direction designed for the lifters. As can be seen from Figure 10, once more, in the 8-lifter mode, due to the bulky lifters and the reduction of the mill volume, as well as the high *KE* of the balls (about 57.43 kJ), the mill wall has been torn and a number of balls have come out of it (115 balls). However, compared to the corresponding mode in the step liner, the *KE* of the balls and the number of balls passing through the mill wall are much less and the mill is in a steadier state. In the 12- and 16-lifter modes, cataract motions as well as appropriate shoulder and toe points for the balls are created, and it can be said that the mill with this lifter count works optimally. In the 20- and 24-lifter modes, cataracting motions gradually disappear, and only cascading motions are observed for the balls. In the 28- to 64-lifter modes, cascade motions also disappear gradually, which indicates that the influence of the lifters on the motions of the balls is decreasing. Therefore, increasing the lifter count to more than 24 lifters is not logical in Step@ liner.

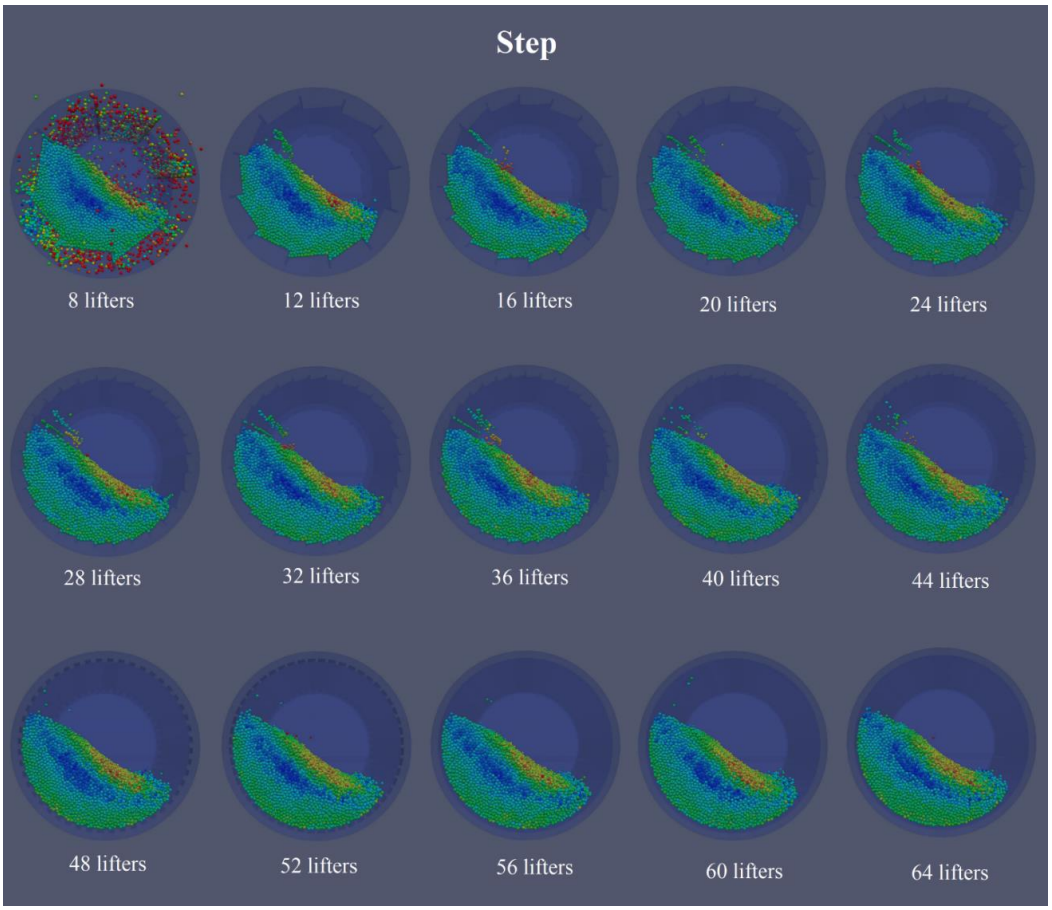

Figure 9. 3D *DEM* simulation snapshots (front view) of industrial ball mills with Step liner from 8 to 64 lifters.

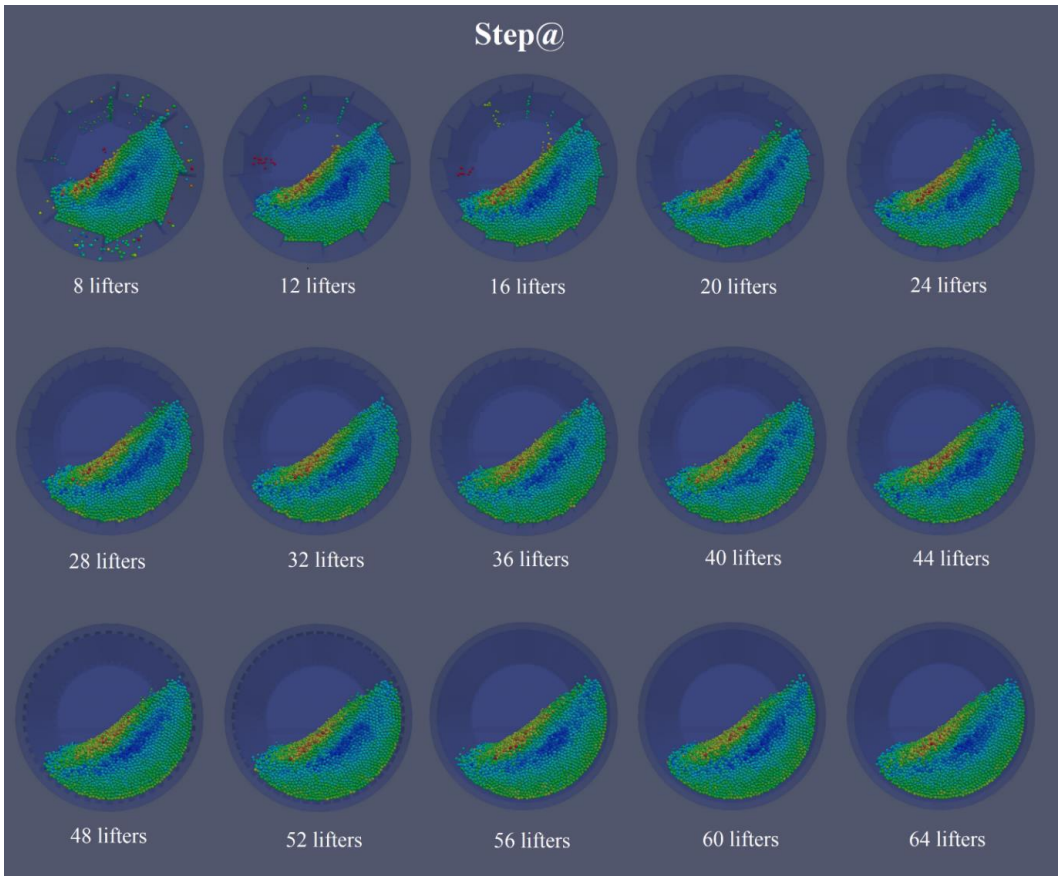

Figure 10. 3D *DEM* simulation snapshots (front view) of industrial ball mills with step@ liner from 8 to 64 lifters.

Figure 11 demonstrates three-dimensional *DEM* simulation snapshots (front view) of industrial ball mills with Ship-lap liner from 8 to 64 lifters. Similar to step liner, the rotation direction of the mill in this liner is of special importance due to its asymmetry. In ship-lap liner, the rotation direction of the mill is opposite to the design of its lifters, and is clockwise. In other words, the direction of rotation of the mill is deliberately chosen incorrectly. On the contrary, in ship-lap@ liner, the direction of rotation of the mill is in accordance with the design of its lifters, and is counter-clockwise (Figure 12). The reason for this work is to compare and investigate the effect of the rotation direction of the mill on the motions of the balls in these asymmetric lifters. As can be seen from Figure 11, in the 8-lifter mode, due to the bulkiness of the lifters (the volume of a single lifter is about 1.311 m^3), the useful volume inside the mill has reached 34.50 m^3 from 44.99 m^3 in the lifter-less mode. That is, it has decreased by about 23%. On the other hand, these bulky lifters bring the *KE* of the balls to about 297.71 kJ in this mode, which is about five and a half times that of the 12-lifter mode (54.76 kJ). As a result, in this mode, the balls have caused the wall of the mill to tear and some of them (2187 balls) have come out of the mill. Therefore, it is practically impossible to install Ship-lap liner with 8 lifters in this mill. Despite the incorrect rotation direction of the mill, due to the edge of its lifters, cascading and cataracting motions have been created for the balls in the 12–24 lifter modes. In the 12-lifter mode, the height of the lifters is such that some of the balls ride on them and rotate with the mill and do not actually participate in the grinding. It can be said that the optimal range for the lifter count in the Ship-lap liner is between 12 and 24 lifters, although the direction of rotation of the mill in this liner is basically wrong. However, in the 28 to 64 lifter modes, cascading and cataracting motions have gradually disappeared, which indicates the insignificant influence of the lifters on the motions of the balls in these modes. In general, it can be said that ship-lap liner similar to Step liner is an appropriate liner for installation in industrial scale ball mills because both its height and width are suitable. Also its edge (unlike the wave liner) creates the required sliding friction between the balls and the lifters.

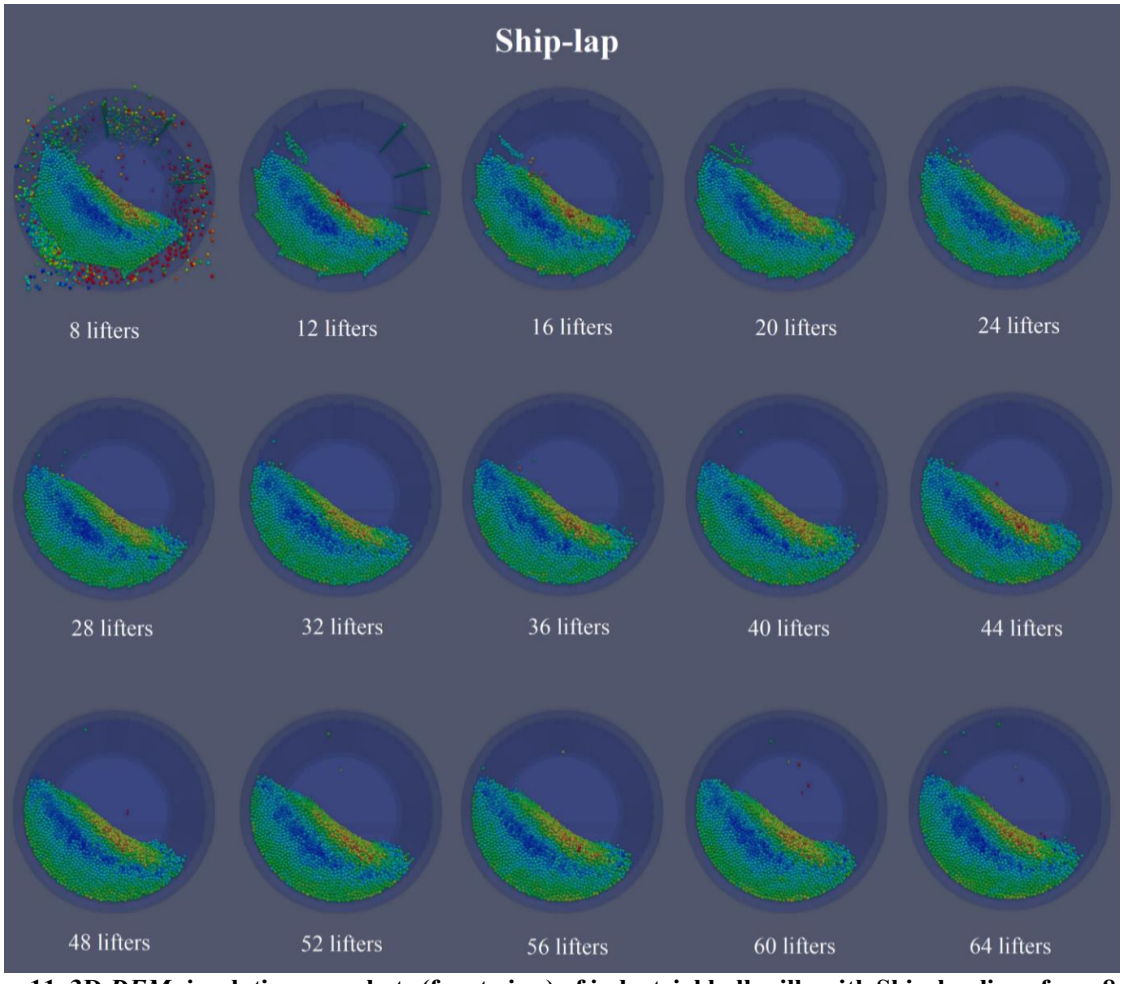

Figure 11. 3D *DEM* simulation snapshots (front view) of industrial ball mills with Ship-lap liner from 8 to 64 lifters.

Figure 12 demonstrates three-dimensional *DEM* simulation snapshots (front view) of industrial ball mills with ship-lap@ liner from 8 to 64 lifters. Ship-lap@ liner in all modes (from 8 to 64 lifters), has the same profile as ship-lap liner. Their difference is in the direction of rotation of the mill. In the Ship-lap@ liner, the mill rotates in the direction designed for the lifters. As can be seen from Figure 12, in the 8-lifter mode, unlike the Ship-lap liner, the *KE* of the balls is such that it does not tear the mill wall (61.30 kJ), and the Ship-lap@ liner performs well in the 8-lifter mode. In the 8-lifter mode, the balls go up to the ceiling of the mill and cataract motions are created for them. However, proper toe points are not created for the balls and they fall on each other in the center of the mill (on the charge profile), which can be attributed to the small lifter count in this mode. To solve this problem, the rotation speed of the mill should be increased in the 8-lifter mode. In 12-, 16-, and 20-lifter modes, the grinding performance is optimal and cascading and cataracting motions, as well as appropriate shoulder and toe points for the balls are created, and it is possible to consider the optimal performance range of ship-lap@ liner between 12 and 20 lifters. In 24-lifter mode, the number of balls lifted by lifters has decreased significantly. In the 28- to 64-lifter modes, the cascading and cataracting motions completely disappear, and it can be said that the lifters do not have the ability to raise the height of the balls. Consequently, it is not recommended to install more than 24 lifters for ship-lap@ liner.

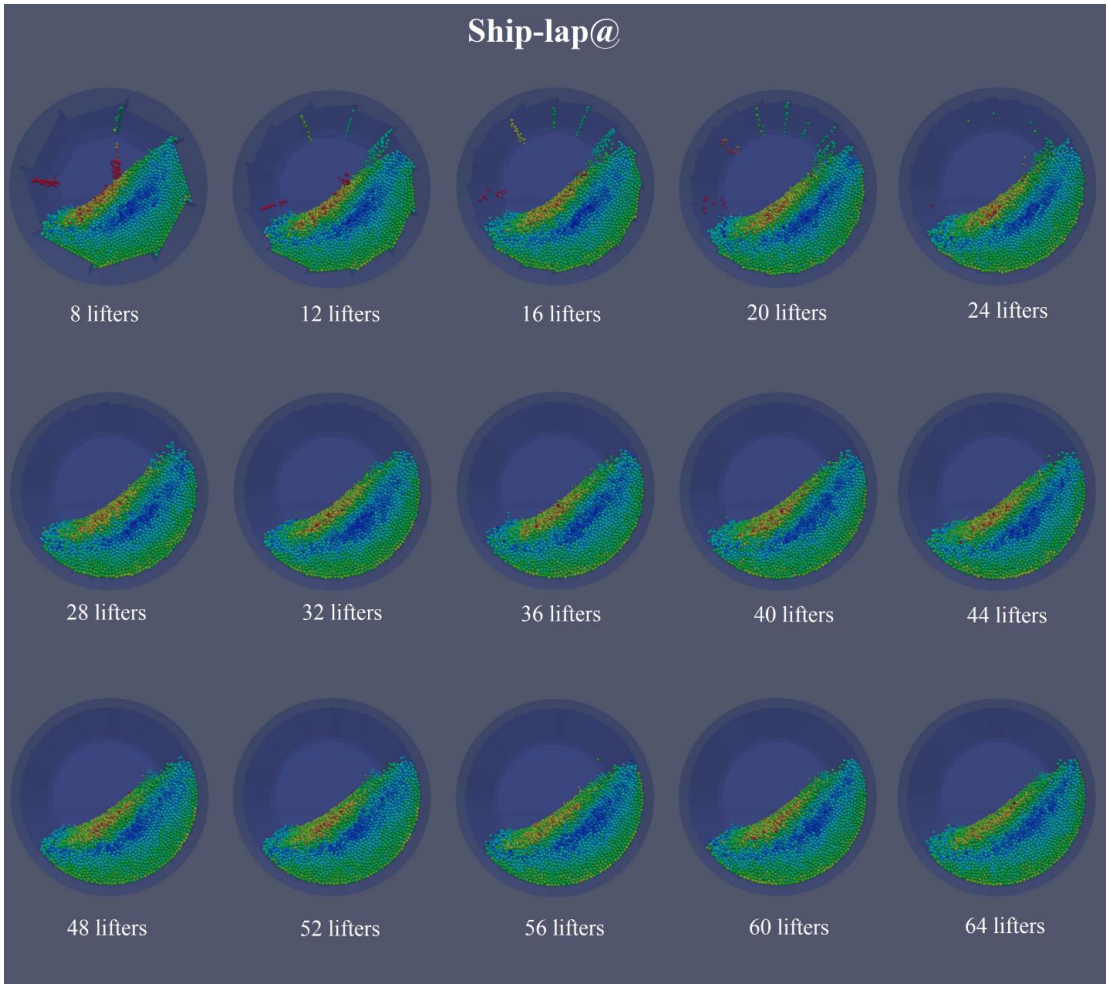

Figure 12. 3D *DEM* simulation snapshots (front view) of industrial ball mills with ship-lap@ liner from 8 to 64 lifters.

3.2. Calculation of *KE*, *PE*, and *TE* of balls for studied liners

In this research work, similar to Part 1, the *KE*, *PE*, and *TE* (*TE* = *KE* + *PE*) of all the balls are calculated and compared throughout the simulation time from zero to thirteen seconds for all the liner types and for all the lifter count mentioned above. This task, i.e., calculating the *KE* and *PE* at each time step, was very laborious and lasted for about two years. Also their corresponding graphs for all

five types of liners and all lifter numbers from eight to sixty-four are drawn and compared in detail (Figs 13 – 18). The *KE*, *PE*, and *TE* have been accurately calculated according to the mass, coordinates, height, and speed of all the balls at any time step according to $KE = 1/2mV^2$, $PE = mgh$, and $TE = KE + PE$ formulas, where, m is the mass of the ball (kg), V is the speed of the ball (m/s), g is the acceleration of gravity (m/s^2), and h is the height of the ball from the bottom of the mill (m). First, the KE_i and PE_i for a single ball (ball i) were calculated (Equations 1 and 2), where m_i is the mass of the ball i (kg), V_i is the speed of the ball i (m/s), and h_i is the height of the ball i from the bottom of the mill (m). Then to calculate the *KE* and *PE* of all the balls, these values were added together (Equations 3 and 4).

$$KE_i = \frac{1}{2} m_i {V_i}^2 \quad (1)$$

$$i = 1, 2, \dots, 79553$$

$$PE_i = m_i g \quad (2)$$

$$i = 1, 2, \dots, 79553$$

$$KE = \sum_{i=1}^{79553} KE_i \quad (3)$$

$$PE = \sum_{i=1}^{79553} PE_i \quad (4)$$

After the mill starts to rotate, first the *KE* and *PE* of the balls increase greatly. After some time, since the mill started working, these energies get to their minimum value. Then, in most mills, they come to a relative steady state in about 3 seconds, which we called steady state 1 (here, 3-13s). But in some mills, it takes about 5 seconds to get to the steady state, which we called steady state 2 (here, 5-13s). To ensure that all mills studied in this research work, with different types of liners and different numbers of lifters, have reached steady state, this final steady state is defined.

Figure 13 demonstrates the values of *KE*, *PE*, *TE*, and their averages for wave liner from 8 to 64 lifters during simulation time from 0 to13s. As can be seen in Figure 13a, after starting the mill, in all modes from 8 to 64 lifters, the *KE* of the balls comes to its first maximum in about 0.5s. Then it gets to its minimum in about 1.2s. One more time, it reaches its second maximum in about 1.5 to 2s. Finally, it comes to a relative stability in about 2.6 to 4s, and in 4.8s, the mill reaches full stability. In the 8- and 12-lifter modes, the *KE* fluctuations are higher than in other modes. Also with the increase in the lifter count, the *KE* of the balls has decreased. In total, the *KE* of the balls in the Wave liner fluctuates between 59 and 76 kJ after the steady state (5–13s). In Figure 13b, after starting the mill, in all modes from 8 to 64 lifters, the *PE* of the balls comes to its maximum in about 1.3s. Then it gets to its minimum in about 2.4s, and finally, in about 3.5s, the amount of fluctuations in the *PE* of the balls decreases, and in 4s, it reaches a relative steady state. Also in the 8-lifter mode, the *PE* of the balls is significantly higher than in other modes. The reason can be attributed to the greater height and width of the lifters in this case. The amount of *PE* fluctuations in the 8-lifter mode is higher than in other modes, which indicates the low lifter count in this mode. In general, similar to the *KE* of the balls, with the increase in the lifter count, their *PE* has decreased. Also the closeness of the graphs in the 20 to 64-lifter modes shows that increasing the lifter count to more than 20 in the wave liner is not logical. On the other hand, in 20- to 64-lifter modes, there is practically no fluctuation in the *PE* of the balls, which indicates that the lifters have no effect on the motions of the balls. The amount of *PE* of the balls in the wave liner fluctuates between 610 and 710 kJ after the steady state (5 to 13s). Figure 13c shows the values of the *TE* of the balls in the 8- to 64-lifter modes from 0 to 13s. As can be seen, the *TE* of the balls has a completely similar trend with their *PE*. Therefore, it can be concluded that the *PE* of the balls has a more important role than their *KE* in the *TE*. The *TE* of the balls in the wave liner fluctuates between 670 and 780 kJ after the steady state (5 to 13s). Figure 13d displays the average *KE* of the balls. As can be seen, with the increase in the lifter count and the decrease in their volume, the amount of *KE* of the balls has decreased, and there is an inverse relationship between them. In fact, as the profile of the lifters shrinks, their impact on the motions of the balls is minimized, and as a result, the *KE* of the balls is reduced. Figure 13e shows the average *PE* of the balls. As can be seen, the *PE* of the balls decreases as the lifter count increases, and their size decreases. In fact, as the lifters get smaller, their ability to lift the balls decreases, and as a result, the *PE* of the balls decreases. In general, there is an inverse relationship between the *PE* of the balls and the increase in the lifter count in the wave liner. This result is contrary to the results of Part 1, where there was a direct relationship between the *PE* of the balls and the lifter count. The reason is that in

Part 1, with the increase in the lifter count, their volume remains constant and their width and height do not change. However, in Part 2 liners, with the increase in the lifter count, their volume decreases drastically. Also Figure 13f shows the average *TE* of the balls in the wave liner. As it is clear, the *TE* of the balls has a completely similar trend with their *PE*, which indicates that the impact of the *PE* on the *TE* of the balls is much greater than their *KE*.

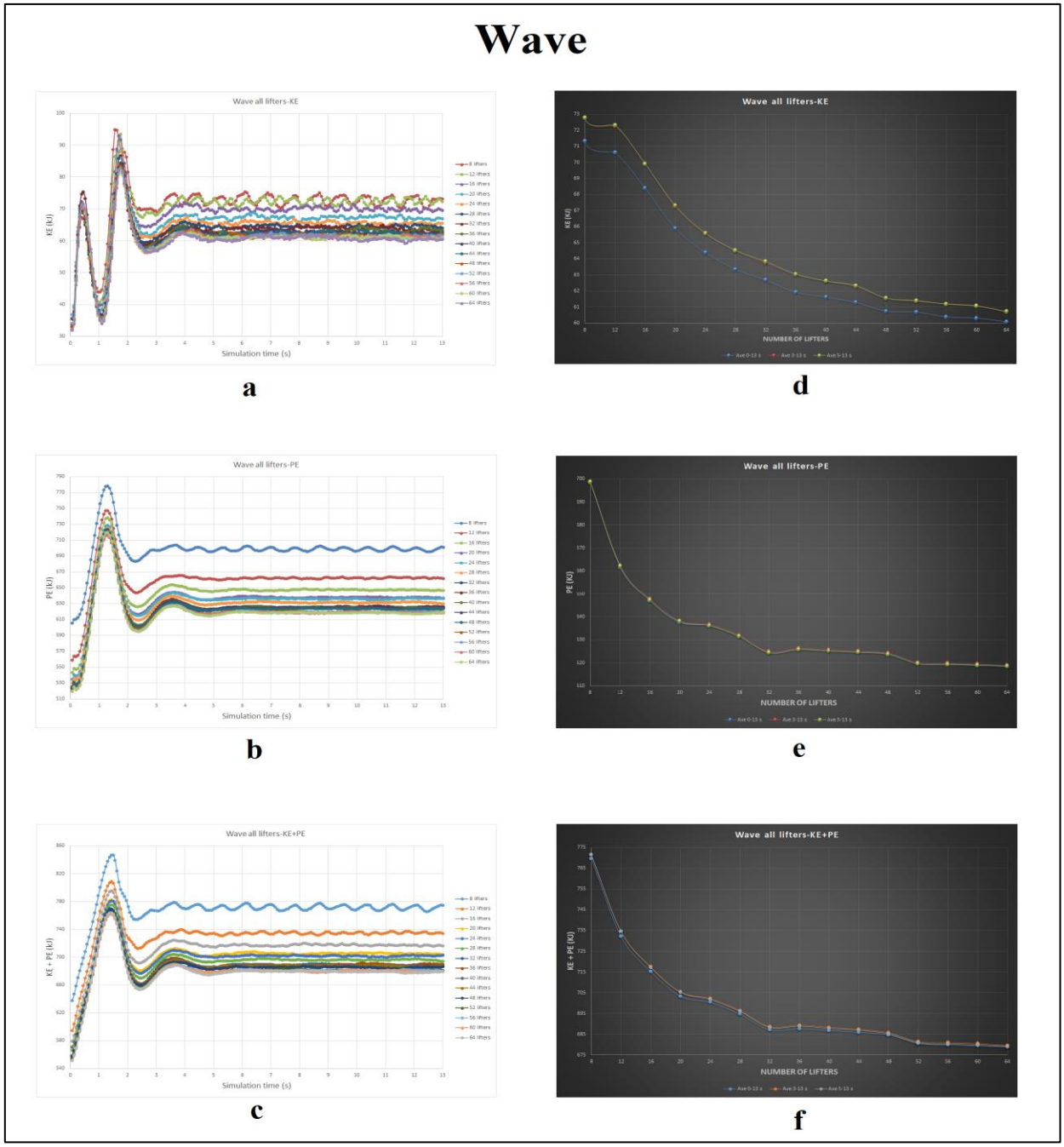

Figure 13. Values of a) *KE* b) *PE* c) *TE* d) the average of *KE* (e) the average of *PE*, and f) the average *TE* of balls for wave liner from 8 to 64 lifters.

Figure 14 demonstrates the values of *KE*, *PE*, *TE*, and their averages for step liner from 12 to 64 lifters during simulation time from 0 to13s. As can be seen in Figure 14a, after starting the mill, in all modes from 12 to 64 lifters, the *KE* of the balls comes to its first maximum in about 0.4s. Then it gets to its minimum in about 1.2s. One more time, it reaches its second maximum in about 1.7 to 1.9 s. Finally, it comes to a relative stability in about 2.8 to 4.2s, and in 5s, the mill reaches full stability. The amount of *KE* fluctuations in all modes from 12 to 64 lifters is almost the same after reaching the

steady state (5 to 13s), which indicates the appropriate lifter count in all modes. In general, the values of *PE* in the step liner fluctuate between 49 and 55 kJ. In Figure 14b, after starting the mill, in all modes from 12 to 64 lifters, the *PE* of the balls comes to its maximum in about 1.4 s. Then it gets to its minimum in about 2.5 s and finally, in about 3.6 s, the amount of fluctuations in the *PE* of the balls decreases and in 5 s, it reaches a relative steady state. As can be seen, the highest *PE* is related to the 12-lifter mode, which indicates the proper height and width of the lifters in this mode. As the lifter count increased, the *PE* of the balls decreased quite regularly. Also, the amount of *PE* fluctuations in all modes is insignificant and the graphs are almost horizontal, which indicates the complete stability of the mill in all modes. In Figure 14c, the *TE* values of the balls are shown. It can be seen that the trend of this graph is almost similar to the *PE* graph, with the difference that the amount of fluctuations in the *TE* is greater than those of the *PE*, which is due to the large fluctuations in the *KE* of the balls. In Figure 14d, the average *KE* of the balls is depicted for the 12- to 64-lifter modes. As can be seen, the *KE* of the balls does not follow a specific trend, and there is no clear relationship between the *KE* of the balls and the lifter count in the step liner. The lowest *PE* of the balls corresponds to the 16-lifter mode (about 49.6 kJ), and the highest *PE* corresponds to the 64-lifter mode (around 54.2 kJ). In Figure 14e, the *PE* values of the balls are depicted. As it can be seen, with the increase in the lifter count from 12 to 64 and the reduction of their size, the *PE* of the balls has decreased from about 740 kJ in the 12-lifter mode to about 615 kJ in the 64-lifter mode, and there is a completely regular trend and an inverse relationship between the *PE* of the balls and the lifter count. Also in Figure 14f, the average values of the *TE* have a completely similar trend to the *PE* of the balls, that is with the increase in the lifter count, the *TE* of the balls has decreased. The reason is that with the decrease in the height and width of the lifters, they practically do not have the ability to raise the balls and increase their speed, and practically the effect of the lifters on the motions of the balls becomes insignificant. It is worth noting that in the step liner, the mill rotates in the wrong direction and against the design of the lifters. By correcting the rotation direction of the mill and matching it with the design of the lifters, the step liner turns into the step@ liner (Figure 15).

Figure 15 demonstrates the values of *KE*, *PE*, *TE*, and their averages for step@ liner from 12 to 64 lifters during simulation time from 0 to13s. As can be seen in Figure 15a, after starting the mill, in all modes from 12 to 64 lifters, the *KE* of the balls comes to its first maximum in about 0.4 to 0.5s. Then it gets to its minimum in about 1 to 1.1s. One more time, it reaches its second maximum in about 1.6 to 1.7 s. Finally, it comes to a relative stability in about 2.6 to 4s, and in 4.8s, the mill reaches full stability. The amount of *KE* fluctuations in all modes is almost the same, which indicates that the lifter count is sufficient in all modes. In general, after the steady state (5 to 13 s), the *KE* of the balls fluctuates from 51 kJ to 56 kJ, which is a small amount. In Figure 15b, after starting the mill, in all modes from 12 to 64 lifters, the *PE* of the balls comes to its maximum in about 1.2s. Then it gets to its minimum in about 2.1 to 2.3s, and finally, in about 3.2 to 3.5s, the amount of fluctuations in the *PE* of the balls decreases and in 4s; it reaches a relative steady state. As can be seen after the second steady state (5–13s), in all modes from 12 to 64 lifters, the *PE* fluctuations are insignificant and the graphs are almost horizontal. The *PE* of the balls in the 12-lifter mode is clearly much higher than other modes, which indicates the appropriate height and width of the lifter in this mode. In the 36 to 64 lifter modes, the graphs are very close to each other, which indicates that increasing the lifter count from 36 lifters and above is not a logical task. The amount of *PE* of the balls after the steady state (5–13s), fluctuates between 610 kJ and 750 kJ (about 140 kJ), which is much more impressive than the *KE* fluctuations (5 kJ). The *TE* values of the balls in Figure 15c have a similar trend with their *PE*. The only difference is that the amount of *TE* fluctuations is slightly higher than the *PE* fluctuations, which is related to the large fluctuations in the *KE* of the balls. In Figure 15d, the average *KE* of the balls for all modes from 12 to 64 lifters is illustrated. As can be seen, there is no special relationship between the *KE* of the balls and the lifter count in the step@ liner, and they are almost independent from each other. In Figure 15e, the average *PE* of balls for all modes from 12 to 64 lifters is shown. As can be seen, with the increase in the lifter count (decrease their volume), the *PE* of the balls decreases regularly, and there is an inverse relationship between them. In Figure 15f, the average *TE* of the balls has a similar trend to their *PE*, which is a confirmation that the role of the *PE* of the balls in their *TE* is much greater than the role of their *KE*. By increase of the lifter count and reduction of their size, the lifters gradually lose the ability to raise the balls and speed them up.

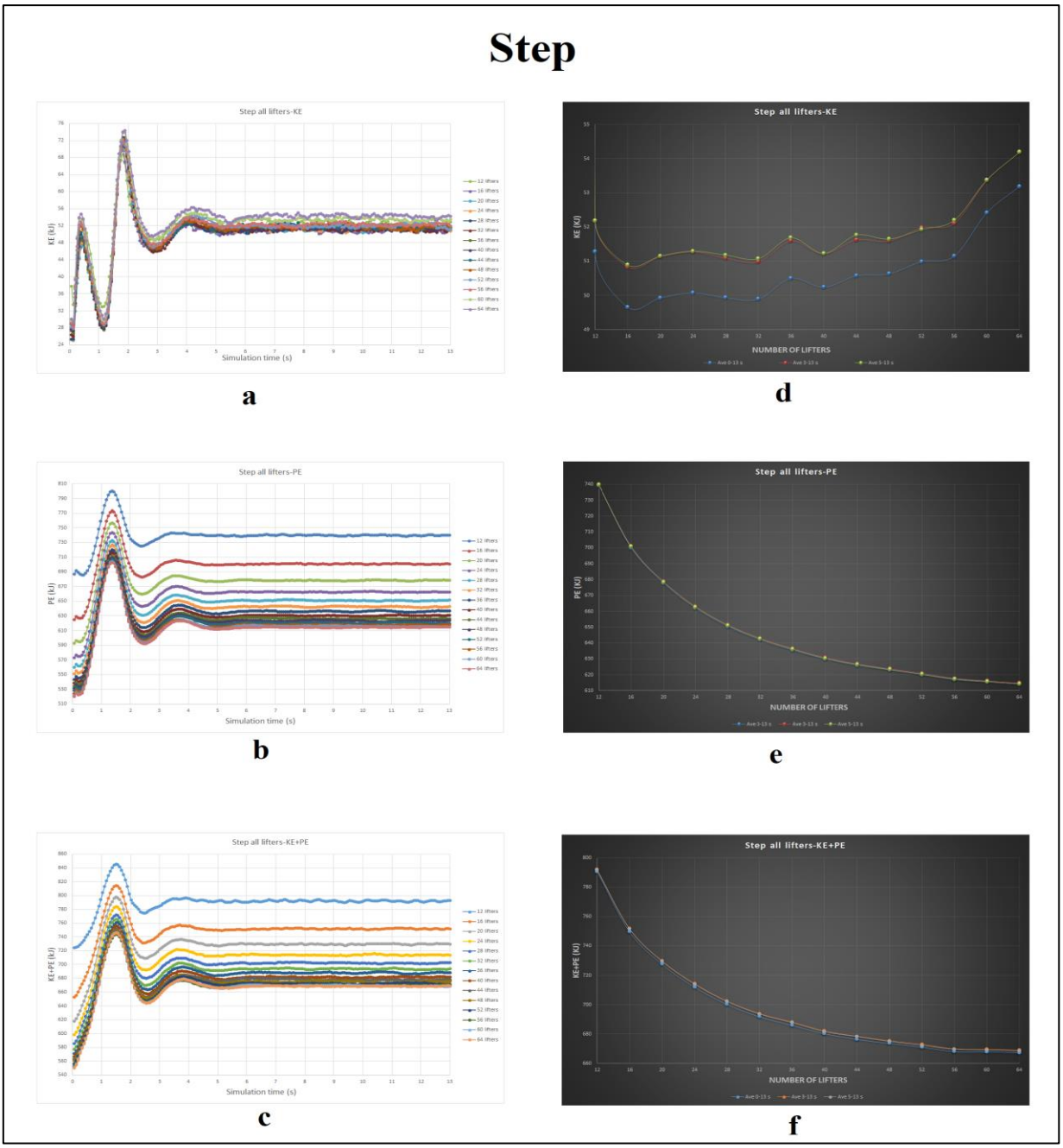

Figure 14. Values of a) *KE* b) *PE* c) *TE* d) the average of *KE* (e) the average of *PE*, and f) the average *TE* of balls for step liner from 12 to 64 lifters.

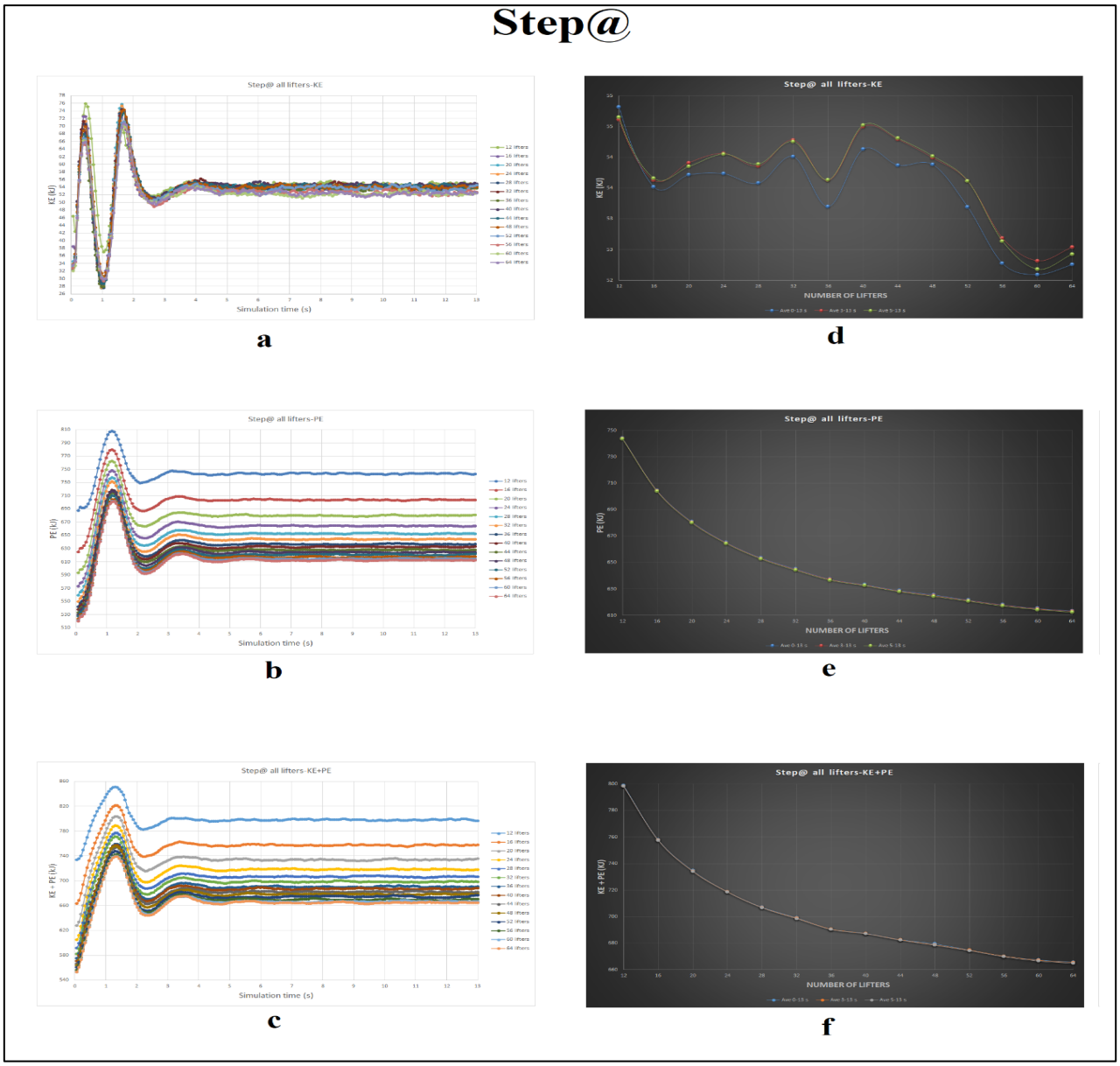

Figure 15. Values of a) *KE* b) *PE* c) *TE* d) the average of *KE* (e) the average of *PE*, and f) the average *TE* of balls for step@ liner from 12 to 64 lifters.

Figure 16 demonstrates the values of *KE*, *PE*, *TE*, and their averages for ship-lap liner from 12 to 64 lifters during simulation time from 0 to13s. As can be seen in Figure 16a, after starting the mill, in all modes from 12 to 64 lifters, the *KE* of the balls come to its first maximum in about 0.5s. Then it gets to its minimum in about 1.2s. One more time, it reaches its second maximum in about 1.7 to 1.9 s. Finally, it comes to a relative stability in about 2.6 to 4.3s, and in 5s, the mill reaches full stability. In the 12-lifter mode, a sudden jump (about 4 kJ) in the *KE* of the balls is observed in 8.4s, which can be attributed to the sudden separation of the balls mounted on the lifter (Figures 11, 12). In other modes, the amount of *KE* fluctuations is almost the same. In general, the *KE* fluctuations for ship-lap liner are about 10 kJ (between 50 and 60 kJ). In Figure 16b, after starting the mill, in all modes from 12 to 64 lifters, the *PE* of the balls comes to its maximum in about 1.3 to 1.4s. Then it gets to its minimum in about 2.3 to 2.5s, and finally, in about 3.4 to 3.6s, the amount of fluctuations in the *PE* of the balls decreases and in 5s, it reaches a relative steady state. The amount of *PE* fluctuations in the 12-lifter mode is higher than in other modes, which is due to a number of balls riding on the lifters and their sudden fall from the lifters. Also in the 12-lifter mode, the distance between the graph and other graphs is more, which indicates the appropriate height and width of the lifter in this mode. From 28 to 64 lifters, the graphs are very close to each other, which indicates that increasing

the lifter count to more than 28 lifters is not logical. In total, the amount of fluctuations in the *PE* of the balls in the ship-lap liner is about 100 kJ (between 580 and 680 kJ), that is about ten times the amount of their *KE* fluctuations. In Figure 16c, it can be seen that the TE of the balls has a behavior similar to their *PE*. The only difference is that the *TE* fluctuates more. In general, the amount of *TE* fluctuations of the balls in the ship-lap liner is between 640 and 730 kJ. In Figure 16d, the relationship between the average *KE* of the balls and the lifter count has been investigated. From 12 lifters to 28 lifters, a decrease in the *KE* of the balls is observed. Then there is an increase in the *KE* of the balls up to the 44-lifter mode. Again, the *KE* decreases up to the 60-lifter mode. In general, there is no significant relationship between the *KE* of the balls and the lifter count in the ship-lap liner. In Figure 16e, unlike the *KE*, there is a clear relationship between the increase in the lifter count, and the decrease in the *PE* of the balls. As the lifter count increases, their volume decreases drastically. As a result, they do not have the ability to raise the balls. In general, there is an inverse relationship between the *PE* of the balls and the lifter count in the Ship-lap liner. In Figure 16f, similar to Figure 16e, the *TE* of balls have also decreased with the increase in the lifter count, which indicates that the *PE* has a greater impact on the *TE* of the balls than the *KE*. It is worth noting that in the ship-lap liner, the mill rotates in the wrong direction and against the design of the lifters. By correcting the rotation direction of the mill and matching it with the design of the lifters, the ship-lap liner turns into the Ship-lap@ liner (Figure 17).

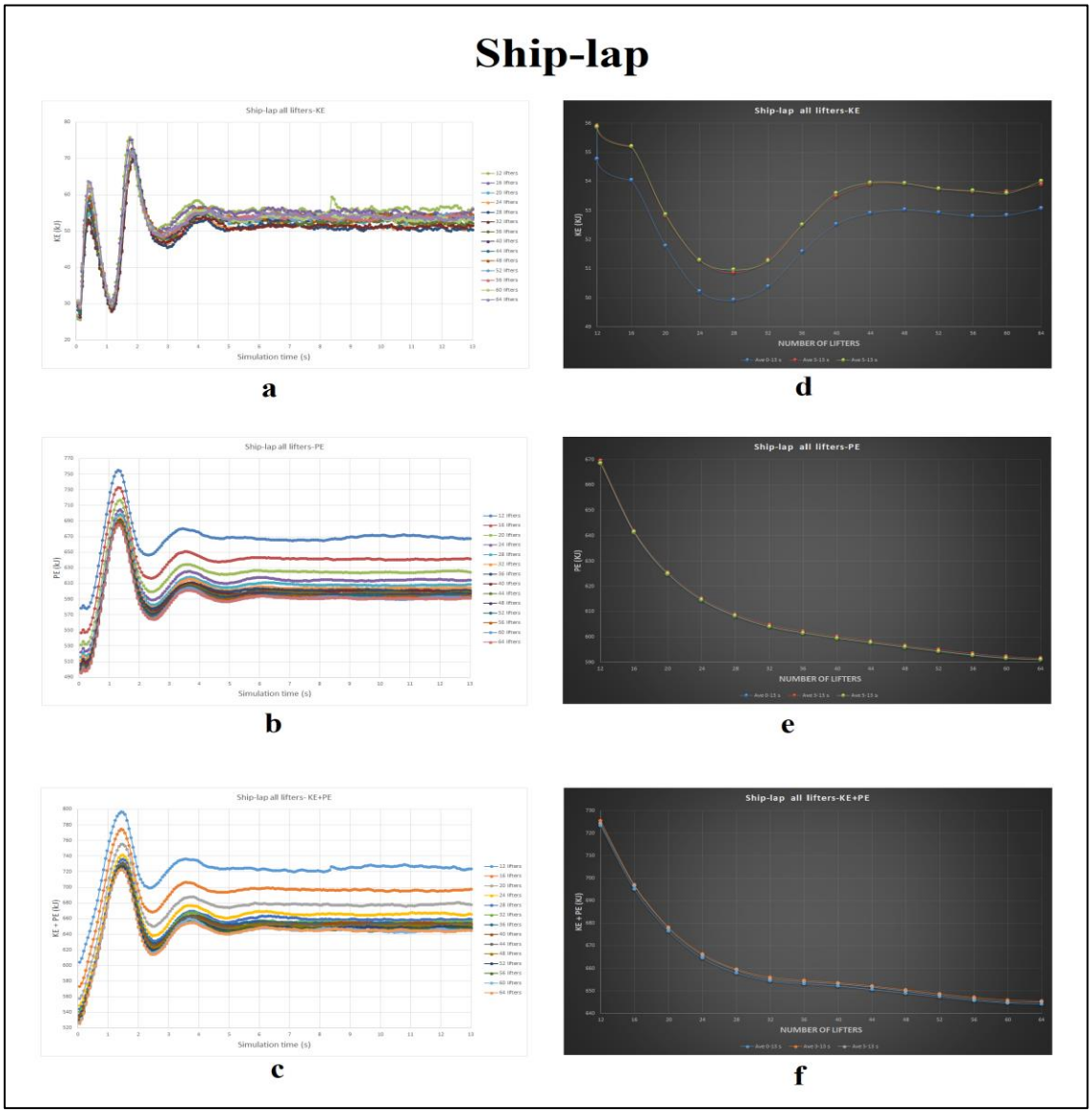

Figure 16. Values of a) *KE* b) *PE*, c) *TE* d) the average of *KE* (e) the average of *PE*, and f) the average *TE* of balls for for the ship-lap liner from 12 to 64 lifters.

Figure 17. demonstrates the values of *KE*, *PE*, *TE*, and their averages for Ship-lap@ liner from 8 to 64 lifters during simulation time from 0 to13 s. In the ship-lap@ liner, unlike the Ship-lap liner, it is possible to install lifters in 8-lifter mode. Also, the volume of the mill in this mode is about 34.50 m^3, which is higher compared to the step@ liner, which reduced the volume of the mill to 24.47 m^3 in the 8-lifter mode. In Figure 17a, after starting the mill, in all modes from 8 to 64 lifters, the *KE* of the balls comes to its first maximum in about 0.5s. Then it gets to its minimum in about 1.1 to 1.2s. One more time, it reaches its second maximum in about 1.6 to 1.7s. Finally, it comes to a relative stability in about 2.5 to 3.7s, and in 5s, the mill reaches a full stability. As can be seen, in the 8-lifter mode, the amount of *KE* fluctuations is higher than other modes, which is due to the small lifter count. In total, the *KE* of the balls in the Ship-lap@ liner fluctuates between 47 and 64 kJ (that is, about 17 kJ), which is a significant amount compared to the other liners studied in Part 2 of this research work. Unlike the ship-lap liner, in the ship-lap@ liner, there is a significant relationship between the *KE* of the balls and the lifter count, and with the increase in the lifter count, their *KE* has decreased. In Figure 17b, after starting the mill, in all modes from 8 to 64 lifters, the *PE* of the balls comes to its maximum in about 1.3 s. Then it gets to its minimum in about 2.1 to 2.4 s and finally, in about 3.4 to 3.5 s, the amount of fluctuations in the *PE* of the balls decreases and in 4.6 s, it reaches a relative steady state. Also, it can be seen that the *PE* diagram of the balls in the 8-lifter mode has a significant distance from the diagram of the other modes and is much higher than them. The reason is that the width and height of the lifters in the 8-lifter mode are greater than in other modes. From 24 to 64 lifters, the graphs are very close to each other, which indicates that increasing the lifter count to more than 24 in the ship-lap@ liner is not logical. After the steady state (5–13s), the graphs are horizontal in all modes and indicates that the lifter count is sufficient, except for the 8-lifter mode, which indicates a small fluctuation in the *PE* of the balls. The amount of *PE* fluctuations in the ship-lap@ liner fluctuates between 580 and 750 kJ (that is, about 170 kJ), which is 10 times the amount of *KE* fluctuations of the balls (17 kJ). Also, with the increase in the lifter count and the rapid decrease in their volume, the *PE* of the balls has decreased drastically, and there is an inverse relationship between them. The *TE* of the balls in Figure 17c has a completely similar trend with their *PE*, which indicates that the *PE* of the balls has a greater effect than their *KE* on the *TE*. In Figure 17d it can be seen that with the increase in the lifter count and the decrease in their volume, the average *KE* of the balls has decreased, and there is an inverse relationship between their *KE* and the lifter count in the ship-lap@ liner. In Figure 17e, with the increase in the lifter count, the average *PE* of the balls has decreased, and there is an inverse relationship between them as well. However, the direction of concavity of the *PE* curve is upward, and it is opposite to the direction of concavity of the *KE* of the balls. In Figure 17f, the average *TE* diagram has a completely similar trend to the average *PE* diagram (Figure 17e), which shows that the role of the balls' *PE* in their *TE* is much stronger.

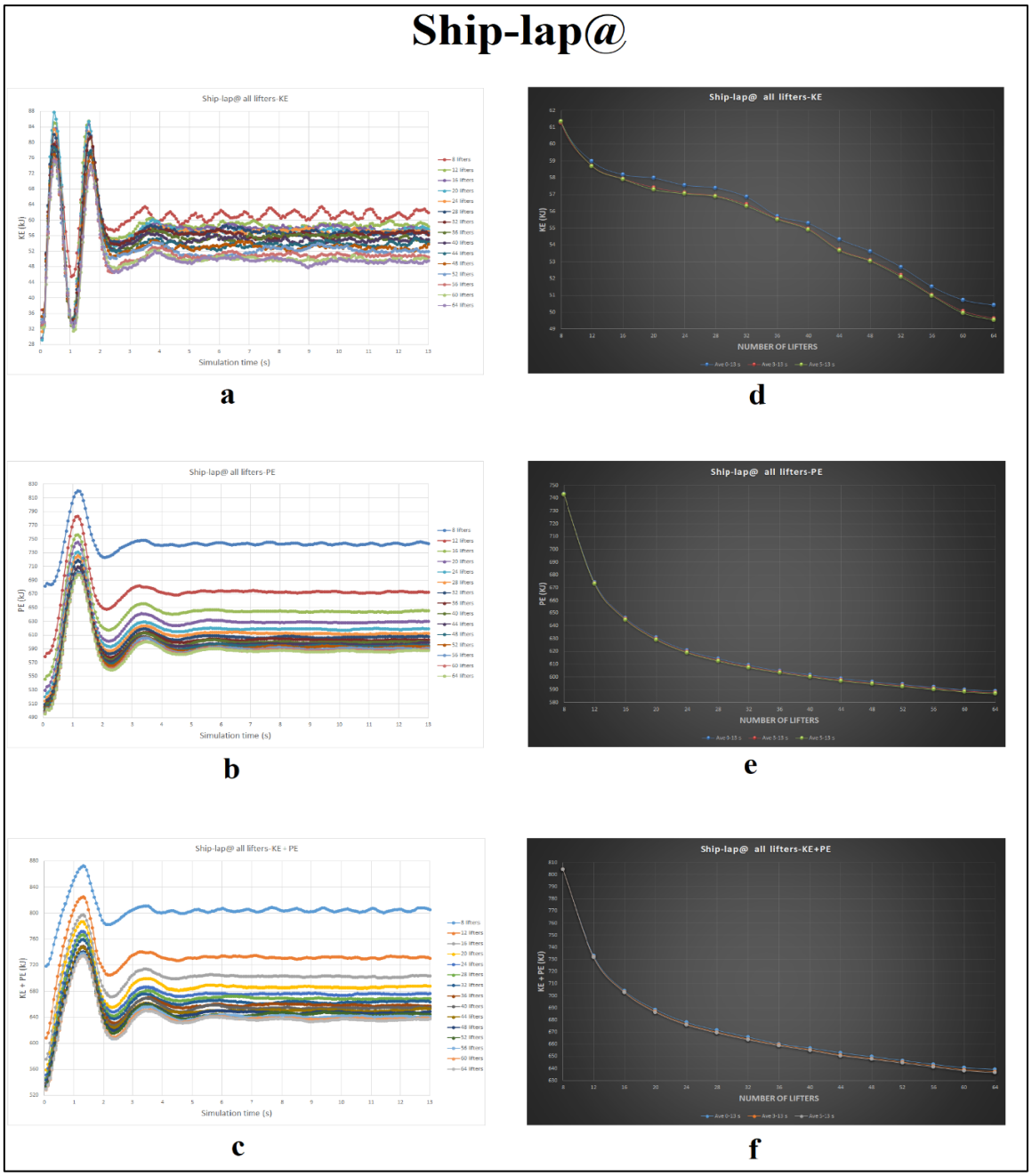

Figure 17. Values of a) *KE*, b) *PE* c) *TE*, d) the average of *KE*, (e) the average of *PE*, and f) the average *TE* of balls for ship-lap@ liner from 8 to 64 lifters

Figure 18 compares the average of the value of *KE* (a), *PE* (b), and *TE* (c) of balls after the second steady state (5-13 s) in all five types of liners studied in this research. In Figure 18a, in the wave liner, as the lifter count (N) increases from 8 to 64, the value of *KE* of the balls (*KE*) decreases binomially according to the following equation:

$$KE_{Wave}\ (kJ) = 0.0053N^2 - 0.5908N + 77.54 \quad (5)$$

$$N = 8, 12, \ldots, 64, R^2 = 0.9834$$

In contrast to the wave liner, in the step liner, as the lifter count (N) increases from 12 to 64; the value of *KE* of the balls increases binomially, according to the following equation:

$$KE_{Step}\ (kJ) = 0.0024N^2 - 0.143N + 53.195 \quad (6)$$

$$N = 12, 16, \ldots, 64, R^2 = 0.8722$$

In the step@ liner, the relationship between the *KE* of the balls and the lifter count (N) is in the form of the following binomial equation:

$$KE_{Step@}\ (kJ) = -0.0015N^2 + 0.0803N + 53.149 \quad (7)$$

N = 12, 16, …, 64, $R^2 = 0.6872$

As can be seen, the coefficient of determination (R^2) in this case is very low, and it can be said that there is no special relationship between the lifter count (N) and the *KE* of the balls in the Step@ liner.

In the ship-lap liner, the relationship between the *KE* of the balls and the lifter count (N) is in the form of the following binomial equation:

$$KE_{\text{Ship-lap}}\,(\text{kJ}) = 0.0036N^2 - 0.267N + 57.396 \quad (8)$$

N = 12, 16, …, 64, $R^2 = 0.359$

As can be seen, one more time, the coefficient of determination (R^2) in this case is too low, and it can be said that there is no special relationship between the lifter count (N) and the *KE* of the balls in the ship-lap liner as well, and in the ship-lap liner, the *KE* of the balls and the lifter count are almost independent from each other.

In the ship-lap@ liner, as the lifter count (N) increases from 8 to 64, the value of *KE* of the balls decreases linearly, according to the following equation:

$$KE_{\text{Ship-lap@}}\,(\text{kJ}) = -0.1881N + 61.778 \quad (9)$$

N = 8, 12, …, 64, $R^2 = 0.9703$

In general, there is an inverse relationship with high R^2 between the *KE* of the balls in the wave and ship-lap@ liners and the lifter count. On the contrary, there is a direct relationship between the *KE* of the balls in the step liner and the lifter count. On the other hand, there is no relationship between the *KE* of the balls in the step@ and ship-lap liners and the lifter count. Therefore, the *KE* of the balls cannot be used to determine the appropriate lifter count, and the *KE* will not be a suitable criterion for this purpose.

In Figure 18b in the wave liner, as the lifter count (N) increases from 8 to 64; the value of *PE* of the balls (*PE*) decreases binomially, according to the following equation:

$$PE_{\text{Wave}}\,(\text{kJ}) = 0.0374N^2 - 3.6623N + 706.43 \quad (10)$$

N = 8, 12, …, 64, $R^2 = 0.8733$

Also in the step liner, as the lifter count (N) increases from 12 to 64, the value of *PE* of the balls decreases binomially, according to the following relationship:

$$PE_{\text{Step}}\,(\text{kJ}) = 0.0625N^2 - 6.7321N + 796.28 \quad (11)$$

N = 12, 16, …, 64, $R^2 = 0.9671$

In the step@ liner, also with the increase in the lifter count (N) from 12 to 64, the *PE* of the balls has decreased binomially, according to the following equation:

$$PE_{\text{Step@}}\,(\text{kJ}) = 0.0615N^2 - 6.7395N + 799.5 \quad (12)$$

N = 12, 16, …, 64, $R^2 = 0.9644$

Also, in the ship-lap liner, with the increase in the lifter count (N) from 12 to 64, the *PE* of the balls has decreased binomially, according to the following equation:

$$PE_{\text{Ship-lap}}\,(\text{kJ}) = 0.0421N^2 - 4.3354N + 701.99 \quad (13)$$

N = 12, 16, …, 64, $R^2 = 0.9339$

Also in the ship-lap@ liner, with the increase in the lifter count (N) from 8 to 64, the *PE* of the balls has decreased in the form of the following power equation:

$$PE_{\text{Ship-lap@}}\,(\text{kJ}) = 860.94N^{-0.097} \quad (14)$$

N = 8, 12, …, 64, $R^2 = 0.8916$

In general, the *PE* of the balls in all the five types of liners investigated in Part 2 of this research work decreases with the increase in the lifter count, and there is an inverse relationship between them (unlike the liners investigated in Part 1 that there was a direct relationship between them). The high coefficient of determination (R^2) between the *PE* of the balls and the lifter count in all five types of liners shows that the *PE* of the balls is a suitable criterion for choosing the optimal lifter count, and should be used as a basis for decision-making.

In Figure 18c, in the wave liner, with the increase in the lifter count from 8 to 64 (N), the *TE* of the balls has decreased binomially, according to the following formula:

$$TE_{\text{Wave}}\,(\text{kJ}) = 0.0427N^2 - 4.2531N + 783.97 \quad (15)$$

N = 8, 12, …, 64, $R^2 = 0.9071$

Also in the step liner, with the increase in the lifter count (N) from 12 to 64, the *TE* of the balls has decreased binomially, according to the equation below:

$$TE_{\text{Step}}\,(\text{kJ}) = 0.0649N^2 - 6.875N + 849.48 \quad (16)$$

N = 12, 16, …, 64, $R^2 = 0.9661$

Also, in the step@ liner, with the increase in the lifter count (N) from 12 to 64, the *TE* of the balls has decreased binomially, according to the following equation:

$$TE_{Step@}\ (kJ) = 0.0601N^2 - 6.6592N + 852.64 \quad (17)$$

N = 12, 16, …, 64, $R^2 = 0.9621$

Also, in the ship-lap liner, with the increase in the lifter count from 12 to 64 (N), the *TE* of the balls has decreased binomially, according to the following formula:

$$TE_{Ship\text{-}lap}\ (kJ) = 0.0457N^2 - 4.6024N + 759.39 \quad (18)$$

N = 12, 16, …, 64, $R^2 = 0.9147$

Also, in the ship-lap@ liner, with the increase in the lifter count from 8 to 64 (N), the *TE* of the balls has decreased in the form of the following power equation:

$$TE_{Ship\text{-}lap@}\ (kJ) = 936.9N^{-0.097} \quad (19)$$

N = 8, 12, …, 64, $R^2 = 0.913$

In general, similar to *PE*, the *TE* of the balls in all the five types of liners investigated in Part 2 of this research work decreases with the increase in the lifter count, and there is an inverse relationship between them (unlike the liners investigated in Part 1 that there was a direct relationship between them). The high coefficient of determination (R^2) between the *TE* of the balls and the lifter count in all the five types of liners shows that the *TE* of the balls is also a suitable criterion for choosing the optimal lifter count, and could be used as a basis for decision-making; this result is contrary to the result obtained in Part 1 of this research, where the *TE* could not be a suitable basis for decision-making.

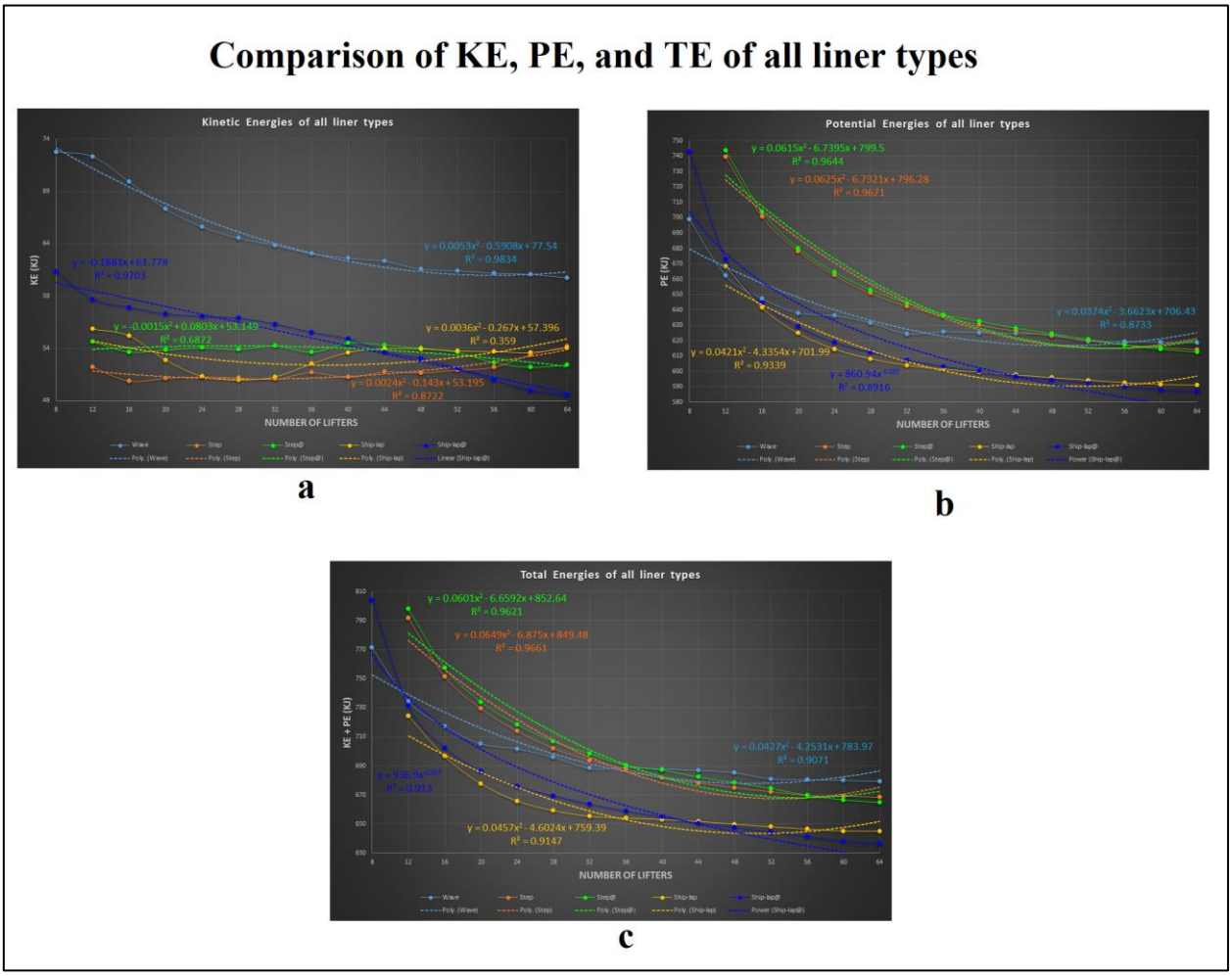

Figure 18. Comparison of the average of the value of *KE* (a) *PE* (b), and *TE* (c) of balls in all five types of liners.

Figure 19 investigates the effect of mill rotation direction on *KE*, *PE*, and *TE* of step, step@, ship-lap, ship-lap@ liners. In Figure 19a, the values of the *KE* of the balls in the step and step@ liners are compared. As can be seen, in the 12- to 56-lifter modes, the *KE* of the balls in the step@ liner is higher than in the step liner, which indicates that if the mill rotates in the right direction according to

the lifter design (step@ mode), lifters can transfer more *KE* to the balls. In the 60- and 64-lifter modes, due to the too small size of the lifters, the results are not logical and as expected. In Figure 19b, the values of the *PE* of the balls in the step and step@ liners are compared. As can be seen, in the 12- to 52-lifter modes, the values of the *PE* in the step@ liner are higher than the step liner, which indicates the importance of the proper direction of rotation in the mill. In the 56 to 64-lifter modes, due to the small size of the lifters, it is not possible for them to raise the balls, and afresh the results obtained are not logical. In Figure 19c, the TE of the balls has a completely similar trend to their *PE*, and in the 12- to 52-lifter modes, the step@ liner, in which the direction of rotation of the mill is in accordance with the design, has shown a better performance. Figure 19d compares the *KE* of the balls in ship-lap and ship-lap@ liners. As can be seen, in the 12- to 40-lifter modes, the ship-lap@ liner, in which the direction of rotation of the mill is according to the design, has a better performance. However, in the 44- to 64-lifter modes, the results are not logical. The reason is that the lifters have a small height and width, and do not have such an effect on the *KE* of the balls. By comparing Figures 19a and 19d, it can be concluded that because the step and step@ liners in all modes from 12 to 64 lifters have more volume (greater height and width) than the corresponding modes in Ship-lap and Ship-lap@ liners, their ineffectiveness occurs in the 56- to 64-lifter modes. But in the ship-lap and ship-lap@ liners, their ineffectiveness occurs in 44- to 64-lifter modes. In other words, if the lifters do not have the proper height and width, the rotation direction of the mill does not have much effect on their performance. Figure 19e compares the *PE* of the balls in the ship-lap and ship-lap@ liners. Once more, in the 12- to 40-lifter modes, the ship-lap@ liner performs better than the ship-lap liner. However, with the shrinking of the width and height of the lifters in the 44- to 64-lifter modes, the obtained results are not logical. Figure 19f compares the *TE* of the balls in ship-lap and ship-lap@ liners. One more time, in the 12- to 40-lifter modes, similar to the *PE*, the *TE* of the balls in the ship-lap@ liner where the mill rotates according to the design of the lifters is higher than in the ship-lap liner. In the 44- to 64-lifter modes, the results are not logical, due to the too small size of the lifters. In other words, when the effect of the lifters on the *PE* and the *TE* of the balls is reduced due to the smallness of the lifters, the direction of rotation of the mill is not important.

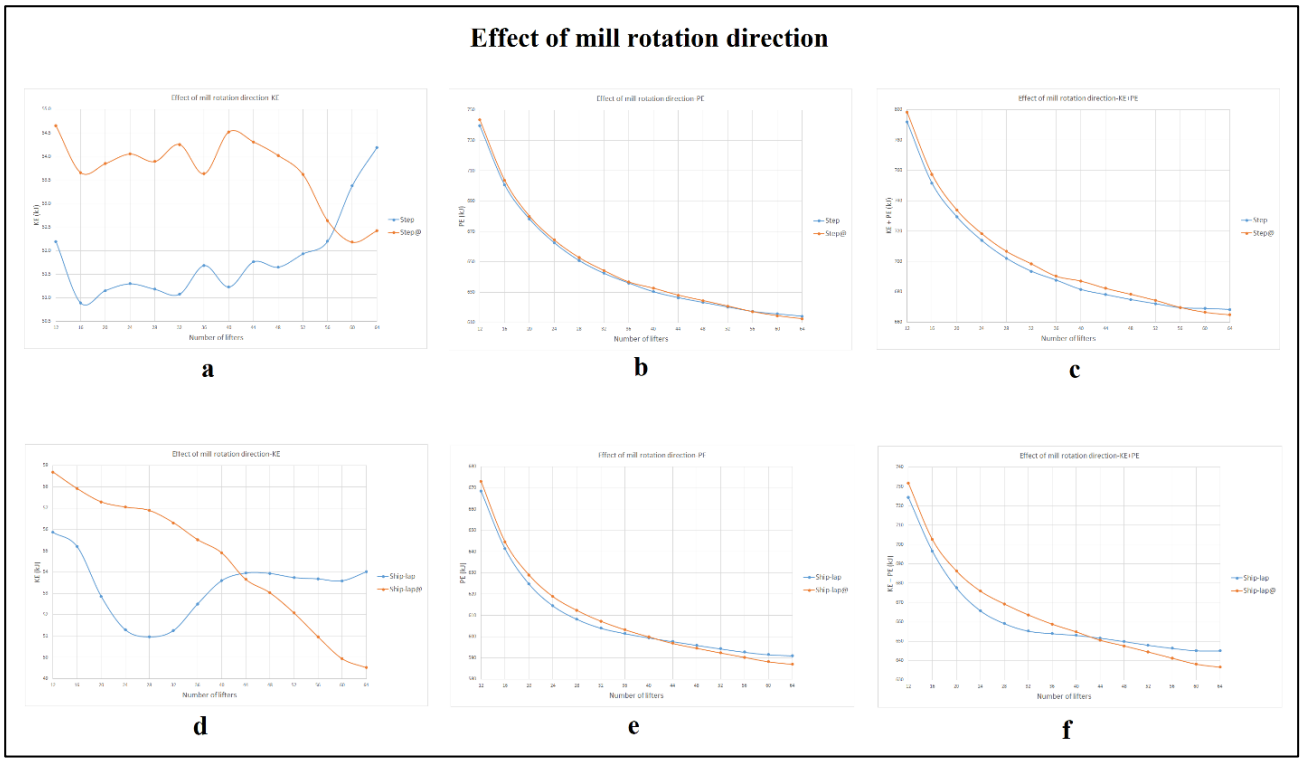

Figure 19. Effect of mill rotation direction on *KE*, *PE*, and *TE* of step, step@, ship-lap, ship-lap@ liners.

6. Investigation of Effect of Mill Rotation Direction on Performance of Meskavan Ball Mill

Validation of simulation results has been done in Part 1 of this research work. Therefore, its repetition has been avoided here. In Part 2, the effect of the direction of mill rotation on the performance of the ball mill of Meskavan Company has been investigated.

In Figure 20, the 3D simulations (front view) of the ball mill of Meskavan Company in two cases of the direction of mill rotation are compared. In case a) (Meskavan), the mill rotates clockwise according to the design of the lifters. But in case b) (Meskavan@), the mill rotates in a trigonometric direction contrary to the design of the lifters. It can be seen that the mill performs well in both cases, and there is no visible difference between the mill's performance in these cases. It can be concluded that the asymmetry in the profile shape of the lifters in the Meskavan mill does not have a significant effect on their performance, and the mill can practically rotate in the desired direction.

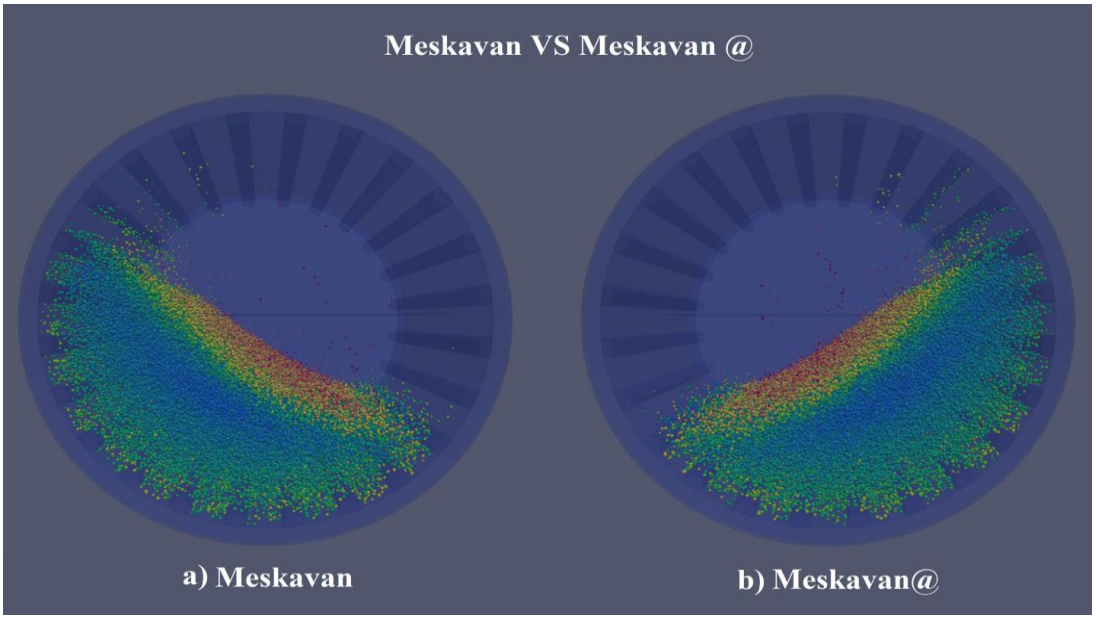

Figure 20. Comparison of *DEM* simulation of Meskavan Company ball mill in two cases: a) rotation of the mill in the clockwise direction and b) rotation of the mill in the counter-clockwise direction.

In Figure 21, the values of *KE*, *PE*, and *TE* of the balls in Meskavan and Meskavan@ mills have been compared. In Figure 21a, it can be seen that after starting of the mills, the *KE* of the balls in both of them has come to its first maximum in about 0.4s. Then it has gotten to its minimum in about 1.2s. Then one more time it has come to its second maximum in about 1.8s. Finally, between 3 and 5s, a relative stability has been reached, and in 5 s, the mills have become completely stable. The graphs of both mills are almost identical, which shows that the direction of mill rotation is ineffective. Also, in Figure 21b, the values of *PE* of the balls in the Meskavan and Meskavan@ mills are compared. As can be seen, after starting the mills, the *PE* of the balls in both of them comes to its maximum in about 1.4 s. Then it gets to its minimum in about 2.7s. Finally, between 2.7 and 4s, it reaches a relative stability state, and in 5s; both mills reach a full stability state. The *PE* values of both mills are almost the same, although surprisingly, the *PE* values of the balls in the Meskavan@ mill are slightly higher than in the Meskavan mill, which indicates that changing the rotation direction of the mill of this company can even improve the mill's performance, although the amount of performance improvement is very small. It can also be seen in Figure 21c that the *PE* values of the balls are much higher than their *KE* values in both Meskavan and Meskavan@ mills. Also, the *TE* values of the balls are closer to their *PE* values, which indicates that the *PE* has a greater effect on the *TE*. In general, there is not much difference in the *KE*, *PE*, and *TE* of the balls in the Meskavan and Meskavan@ mills. Therefore, it can be concluded that making the Meskavan mill lifter profile asymmetric has not affected its performance. In order to improve the performance of the Meskavan mill, the asymmetry of the lifter profile should be increased.

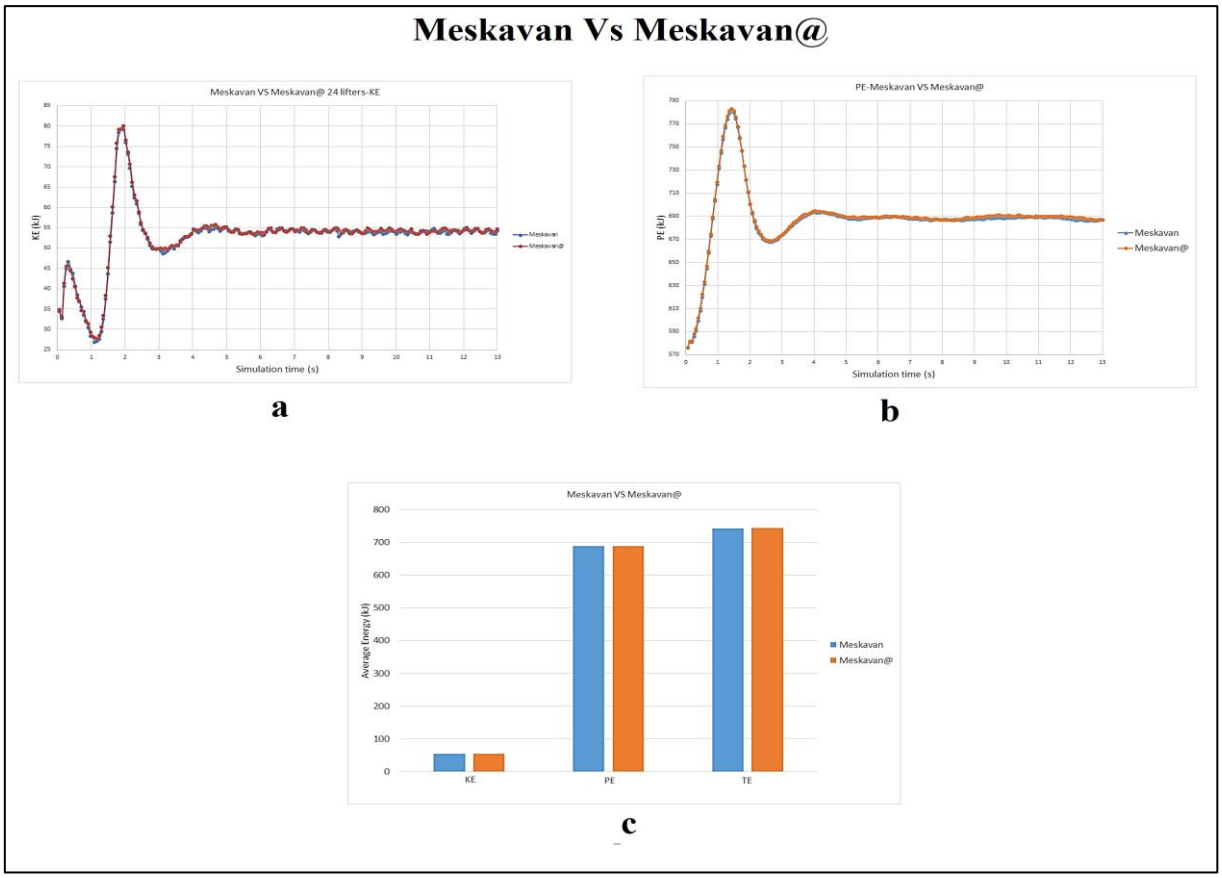

Figure 21. Comparison of *KE*, *PE*, and *TE* values of the ball mill of Meskavan Company in two cases: clockwise (Meskavan) and counter-clockwise (Meskavan@).

7. Conclusions

In this research work, similar to Part 1, the *KE*, *PE*, and *TE* of all the balls inside a good many of industrial-scale ball mills were calculated in the entire duration of the *DEM* simulations from 0 to 13s. In Part 2 of this research work, five types of liners i.e. wave, step, step@, ship-lap, and ship-lap@, were examined. Unlike the Part 1 liners, whose lifters were separate and their volume did not change with the increase in the lifter count, the Part 2 liners all had similar connected lifters with different volumes and as the lifter count increased, their volume decreased drastically. Also, their corresponding graphs for all the five types of liners and all lifter numbers from eight to sixty-four were drawn and compared in details. On the other hand, using data related to these energies, for each type of liner, the optimal lifter count was obtained. Also the effect of mill rotation direction on the values of *KE*, *PE*, and *TE* of balls in step, ship-lap, and Meskavan liners was investigated.

Also, the following practical and valuable results were obtained from this research work:

- Similar to Part 1, when the *KE* of the balls has less fluctuations, the number of mill lifters is suitable. On the contrary, when the fluctuations of *KE* are high, it indicates that the lifter count is not enough and the motion of the balls in the mill is not uniform and stable. Also, from the fluctuations of the *PE* of the balls, it is possible to find out whether the lifter count is sufficient or not.
- Similar to Part 1, in all cases, the *PE* values were significantly higher than the *KE* values, which indicates that *PE* is much more important than *KE,* and should be the basis of analysis and lifters, which can raise the balls to a higher height are more appropriate.
- Wave liner is not suitable for installation in industrial ball mills due to the inability to create an impact mechanism for the balls. However, in some industries such as the cement industry, where an abrasion mechanism is required and the production of fines does not cause problems for the next stages of the process, this liner can be used.
- Step and ship-lap liners are appropriate liners for installation in industrial scale ball mills, because both their height and width are suitable. Also their edge creates the required sliding friction between the balls and the lifters.
- In the wave liner, there was an inverse relationship between the *PE* of the balls and the

increase of the lifter count. This result was contrary to the results of Part 1, where there was a direct relationship between the *PE* of the balls and the lifter count. The reason is that in Part 1, with the increase of the lifter count, their volume remained constant, and their width and height did not change. However, in the Part 2 liners, with the increase of the lifter count, their volume decreased drastically.

- In general, there was an inverse relationship with high R^2 between *KE* in the wave and ship-lap@ liners and the lifter count. On the contrary, there was a direct relationship between *KE* in the step liner and the lifter count. On the other hand, there was no relationship between *KE* in the step@ and ship-lap liners and the lifter count. Therefore, *KE* cannot be used to determine the appropriate lifter count, and it is not a suitable criterion for this purpose.
- In general, *PE* in all five types of liners investigated in Part 2 decreased with the increase of the lifter count, and there was an inverse relationship between them (unlike liners investigated in Part 1 that there was a direct relationship between them).
- The high coefficient of determination (R^2) between *PE* and the lifter count in all five types of liners showed that *PE* is a suitable criterion for choosing the optimal lifter count and should be used as a basis for decision making.
- The high coefficient of determination (R^2) between *TE* and the lifter count in all five types of liners shows that *TE* is also a suitable criterion for choosing the optimal lifter count and could be used as a basis for decision making (This result is contrary to the result obtained in Part 1 of this research, where *TE* could not be a suitable basis for decision making.)
- If the lifters do not have the proper height and width, the rotation direction of the mill does not have much effect on their performance. In other words, when the effect of the lifters on the *PE* and the TE of the balls is reduced due to the smallness of the lifters, the direction of rotation of the mill is not important.
- It was shown that Step@ and Ship-lap@ liners transfer more energy to the balls than Step and Ship-lap liners and had a suitable direction of rotation.
- By using data related to *KE*, *PE*, and *TE*, the optimal lifter count was obtained. Accordingly, 8 to 16 lifters were recommended for the Wave liner, 12 to 20 lifters for the Step, Step@, and Ship-lap liners, and 8 to 20 lifters for the Ship-lap@ liner.
- It can be concluded that the asymmetry in the profile shape of the lifters in the Meskavan mill does not have a significant effect on their performance and the mill can practically rotate in the desired direction.
- In general, there was not much difference in the *KE*, *PE*, and *TE* of the balls in the Meskavan and Meskavan@ mills. Therefore, it can be concluded that making the Meskavan mill lifter profile asymmetric has not affected its performance. In order to improve the performance of the Meskavan mill, the asymmetry of the lifter profile should be increased.

Acknowledgements

The authors would like to thank Shahrood University of Technology and Meskavan Company (Abbas Abad, Shahrood) for their support.

References

[1]. Rosales-Marín, G., Andrade, J., Alvarado, G., Delgadillo, G.A., & Tuzcu, E.T. (2019). Study of lifter wear and breakage rates for different lifter geometries in tumbling mill: Experimental and simulation analysis using population balance model. *Minerals Engineering, 141*, 105857.

[2]. Pedrayes, F., Norniella, J.G., Melero, M.G., Menéndez-Aguado, J.M., Juan, J.J., & del Coz-Díaz, J. (2018). Frequency domain characterization of torque in tumbling ball mills using DEM modelling: Application to filling level monitoring. *Powder Technology, 323,* 433–444.

[3]. Mishra, B.K. (2003a). A review of computer simulation of tumbling mills by the discrete element method: Part I— contact mechanics. *International Journal of Mineral Processing, 71,* 73– 93.

[4]. Cleary, P.W. (2001b). Modelling comminution devices using DEM. *International Journal for numerical and analytical methods in geomechanics, 25,* 83–105.

[5]. Góralczyk, M., Krot, P., Zimroz, R., & Ogonowski, S. (2020). Increasing energy efficiency and productivity of the comminution process in tumbling mills by indirect measurements of internal dynamics—an overview. *Energies, 13,* 6735.

[6]. Monama, G.M., & Moys, M.H. (2002). DEM modelling of the dynamics of mill startup. *Minerals Engineering, 15,* 487–492.

[7]. Makokha, A.B., Moys, M.H., Bwalya, M.M., & Kimera, K. A new approach to optimising the life and performance of worn liners in ball mills: Experimental study and DEM simulation. *International Journal of Mineral Processing, 84,* 221–227.

[8]. Yahyaei, M., Powel, M.S., Toor, P., Tuxford, A., & Limpus, A. (2015). Relining efficiency and liner design for improved plant performance. *Minerals Engineering, 83,* 64–77.

[9]. Mishra, B.K. (2003b). A review of computer simulation of tumbling mills by the discrete element method: Part II—Practical applications. *International Journal of Mineral Processing, 71,* 95–112.

[10]. Rajamani, R.K., Rashidi, S., & Dhawan, N. (2014). Advances in discrete element method application to grinding mills. *Mineral Processing and Extractive Metallurgy, 100,* 117–128.

[11]. Mishra, B.K., & Rajamani, R.K. (1992). The discrete element method for the simulation of ball mills. *Applied Mathematical Modelling, 16(11),* 598–604.

[12]. Mishra, B.K., & Rajamani, R.K. (1993). Numerical simulation of charge motion in ball mills—Lifter bar effect. *Mining, Metallurgy & Exploration, 10,* 86–90.

[13]. Mishra, B.K., & Rajamani, R.K. (1994a). Simulation of charge motion in ball mills. Part 1: experimental verifications. *International Journal of Mineral Processing, 40,* 171–186.

[14]. Mishra, B.K., & Rajamani, R.K. (1994b). Simulation of charge motion in ball mills. Part 2: numerical simulations. *International Journal of Mineral Processing, 40,* 187–197.

[15]. Agrawala, S., Rajamani, R.K., Songfack, P., & Mishra, B.K. (1997). Mechanics of media motion in tumbling mills with 3d discrete element method. *Minerals Engineering, 10(2),* 215–227.

[16]. Radziszewski, P. (1999). Comparing three DEM charge motion models. *Minerals Engineering, 12(12),* 1501–1520.

[17]. Cleary, P.W. (1998). Predicting charge motion, power draw, segregation and wear in ball mills using discrete element methods. *Minerals Engineering, 11,* 1061–1080.

[18]. Cleary, P.W. (2001a). Charge behaviour and power consumption in ball mills: sensitivity to mill operating conditions, liner geometry and charge composition. *International Journal of Mineral Processing, 63,* 79–114.

[19]. Hlungwani, O., Rikhotso, J., Dong, H., & Moys, M.H. Further validation of DEM modeling of milling: effects of liner profile and mill speed. *Minerals Engineering, 16,* 993–998.

[20]. Djordjevic, N. (2003a). Discrete element modelling of the influence of lifters on power draw of tumbling mills. *Minerals Engineering, 16,* 331–336.

[21]. Djordjevic, N. (2003b). Discrete element modelling of power draw of tumbling mills. *Mineral Processing and Extractive Metallurgy, 112(2),* 109–114.

[22]. Djordjevic, N. (2003c). Discrete element modelling of lifter stresses in tumbling mill. *Mineral Processing and Extractive Metallurgy, 112(2),* 115–119.

[23]. Powell, M.S., & McBride, A.T. (2004). A three-dimensional analysis of media motion and grinding regions in mills. *Minerals Engineering, 17,* 1099–1109.

[24]. Makokha, A.B., & Moys, M.H. (2006). Towards optimising ball-milling capacity: Effect of lifter design. *Minerals Engineering, 19,* 1439–1445.

[25]. Rezaeizadeh, M., Fooladi, M., Powell, M.S., & Mansouri, S.H. Experimental observations of lifter parameters and mill operation on power draw and liner impact loading. *Minerals Engineering, 23,* 1182–1191.

[26]. Pérez-Alonso, C., & Delgadillo, J.A. (2012). Experimental validation of 2D DEM code by digital image analysis in tumbling mills. *Minerals Engineering,* 25, 20–27.

[27]. Bbosa, L.S., Govender, I., & Mainza, A. (2016). Development of a novel methodology to determine mill power draw. *International Journal of Mineral Processing, 149,* 94–103.

[28]. Boemer, D., & Ponthot, J.P. (2017). DEM modeling of ball mills with experimental validation: influence of contact parameters on charge motion and power draw. *Computational Particle Mechanics 2017, 4,* 53–67.

[29]. Peng, Y., Li, T., Zhu, Z., Zou, S., & Yin, Z. (2017). Discrete element method simulations of load behavior with mono-sized iron ore particles in a ball mill. *Advances in Mechanical Engineering, 9(5),* 1687814017705597.

[30]. Bian, X., Wang, G., Wang, H., Wang, S., & Lv, W. (2017). Effect of lifters and mill speed on particle behaviour, torque, and power consumption of a tumbling ball mill: Experimental study and DEM simulation. *Minerals Engineering, 105,* 22–35.

[31]. Sun, Y., Liang, M., Jin, X., Ji, P., & Shan, J. (2017). Experimental and modeling study of the regular polygon angle-spiral liner in ball mills. *Chinese Journal of Mechanical Engineering, 30(2),* 363–372.

[32]. Yin, Z., Peng, Y., Zhu, Z., Yu, Z., & Li, T. (2017). Impact load behavior between different charge and lifter in a laboratory-scale mill. *Materials, 10(8),* 882.

[33]. Li, Z., Wang, Y., Li, K., Lin, W., & Tong, X. (2018). Study on the performance of ball mill with liner structure based on DEM. *Journal of Engineering & Technological Sciences, 50(2)*.

[34]. Panjipour, R., & Barani, K. (2018). The effect of ball size distribution on power draw, charge motion and breakage mechanism of tumbling ball mill by discrete element method (DEM) simulation. *Physicochemical Problems of Mineral Processing, 54(2),* 258-269.

[35]. Lee, H., Kim, K., & Lee H. Analysis of grinding kinetics in a laboratory ball mill using population-balance-model and discrete-element-method. *Advanced Powder Technology, 30,* 2517–2526.

[36]. Li, G., Roufail, R., Klein, B., Zhou, L., Kumar, A., Sun, C., Kou, J., & Yu, L. (2019). Investigations on the charge motion and breakage effect of the magnetic liner mill using DEM. *Mining, Metallurgy & Exploration, 36,* 1053–1065.

[37]. Chimwani, N., & Bwalya, M.M. (2020). Using DEM to investigate how shell liner can induce ball segregation in a ball mill. *Minerals Engineering, 151,* 106311.

[38]. Shahbazi, B., Jafari, M., Parian, M., Rosenkranz, J., & Chehreh Chelgani, S. (2020). Study on the impacts of media shapes on the performance of tumbling mills – A review. *Minerals Engineering, 157,* 106490.

[39]. AmanNejad, M., & Barani, K. (2021). Effects of Ball Size Distribution and Mill Speed and Their Interactions on Ball Milling Using DEM. *Mineral Processing and Extractive Metallurgy Review, 42(6),* 374–379.

[40]. Kolahi, S., Jahani Chegeni, M., & Seifpanahi-Shabani, K. (2021). Investigation of the effect of industrial ball mill liner type on their comminution mechanism using DEM. *International Journal of Mining and Geo-Engineering, 55(2),* 97–107.

[41]. Jahani Chegeni, M., & Kolahi, S. (2021). Determining an Appropriate range for the Number of Cuboid Lifters in Ball Mills using DEM. *Journal of Mining and Environment, 12(3),* 845–862.

[42]. Safa, A., & Sahraoui, A. (2023). Exploring the effects of a new lifter design and ball mill speed on grinding performance and particle behaviour: A comparative analysis. *Engineering and Technology Journal, 41*(07).

Appendix 1

Due to the file upload size limitation in JME (25 MB), click on the links below to see the high-resolution images and videos of the simulations.
https://s32.picofile.com/file/8477683426/images_part_2_JME.rar.html
https://s32.picofile.com/file/8477683492/videos_part_2_JME.rar.html

انجمن مهندسی معدن ایران
نشریه مهندسی معدن و محیط زیست
نشانی نشریه: www.jme.shahroodut.ac.ir
دانشگاه صنعتی شاهرود

بررسی اثر نوع لاینر و تعداد لیفتر بر انرژی‌های جنبشی، پتانسیل و کل واسطه¬های آسیاکنی در آسیاهای گلوله‌ای صنعتی - قسمت ۲: لیفترهای متصل مشابه با حجم‌های مختلف

سجاد کلاهی، محمد جهانی چگنی* و اصغر عزیزی

دانشکده مهندسی معدن، نفت و ژئوفیزیک، دانشگاه صنعتی شاهرود، شاهرود، ایران

اطلاعات مقاله

تاریخ ارسال: ۲۰۲۴/۰۶/۲۴
تاریخ داوری: ۲۰۲۴/۱۱/۲۷
تاریخ پذیرش: ۲۰۲۵/۰۱/۱۰

DOI: 10.22044/jme.2025.14803.2809

کلمات کلیدی

روش اجزای گسسته
آسیاب‌های گلوله‌ای صنعتی
نوع لاینر
تعداد بالابرها
انرژی‌های جنبشی و پتانسیل

چکیده

در قسمت دوم این کار تحقیقاتی، پنج نوع لاینر یعنی موجی، استپ، استپ@، شیپ-لپ و شیپ-لپ@ مورد بررسی قرار گرفته¬اند. این لاینرها همگی لیفترهای متصل مشابه با حجم¬های متفاوت دارند. تفاوت آن¬ها در عرض، ارتفاع و نوع پروفیل لیفتر است. تمام پنج نوع لاینر، از ۸ تا ۶۴ لیفتر، با استفاده از روش اجزای گسسته (راگ) شبیه¬سازی شده¬اند. در این کار تحقیقاتی برای اولین بار از داده¬های حاصل از مجموع انرژی¬های جنبشی و پتانسیل تک¬تک گلوله¬ها (۷۹۵۵۳ ذره) برای یافتن محدوده مناسب برای تعداد لیفترها استفاده شده است. به عبارت دیگر، انرژی¬های جنبشی و پتانسیل تمام ذرات درون سیستم (داخل آسیای گلوله¬ای) مبنایی برای تعیین تعداد مناسب لیفترها هستند. نتایج نشان می‌دهند که برای لاینر موجی، محدوده مناسب تعداد لیفترها بین ۸ تا ۱۶ است، برای لاینرهای استپ، استپ@، و شیپ-لپ بین ۱۲ تا ۲۰ است و برای لاینر شیپ-لپ@ بین ۸ تا ۲۰ است. در واقع با استفاده از داده¬های انرژی¬های جنبشی و پتانسیل گلوله¬های داخل آسیا می¬توان محدوده مناسب تعداد لیفترها را تعیین کرد که برای اولین بار در این تحقیق انجام شده است. به طور کلی، پیشنهاد می‌شود که از داده‌های انرژی جنبشی و پتانسیل گلوله‌ها برای تعیین تعداد لیفترهای آسیا استفاده شود و برخلاف آنچه تاکنون توسط محققان دیگر انجام شده است، تعداد لیفترهای آسیا را نباید صرفاً با استفاده از قطر آن یا ابعاد لیفترها تعیین کرد. همچنین تأثیر جهت چرخش آسیا بر مقادیر انرژی¬های جنبشی و پتانسیل در لاینرهای استپ و شیپ-لپ بررسی شده است. نشان داده شده است که لاینرهای استپ@ و شیپ-لپ@ انرژی بیشتری نسبت به لاینرهای استپ و شیپ-لپ به گلوله¬ها منتقل می¬کنند و جهت چرخش مناسبی دارند.

نویسنده مسئول مکاتبات: M.Jahani@shahroodut.ac.ir (م. جهانی چگنی)